

Industrial Ziegler-Type Hydrogenation Catalysts Made from Co(neodecanoate)₂ or Ni(2-ethylhexanoate)₂ and AlEt₃: Evidence for Nanoclusters and Sub-Nanocluster or Larger Ziegler-Nanocluster Based Catalysis

William M. Alley,[†] Isil K. Hamdemir,[†] Qi Wang,[‡] Anatoly I. Frenkel,[‡] Long Li,[§] Judith C. Yang,[§] Laurent D. Menard,^{||} Ralph G. Nuzzo,^{||} Saim Ozkar,[⊥] Kuang-Hway Yih,[#] Kimberly A. Johnson,[¶] and Richard G. Finke^{*,†}

[†]Department of Chemistry, Colorado State University, Fort Collins, Colorado 80523, United States

[‡]Department of Physics, Yeshiva University, New York, New York 10016, United States

[§]University of Pittsburgh, Pittsburgh, Pennsylvania 15261, United States

^{||}University of Illinois, Urbana, Illinois 61801, United States

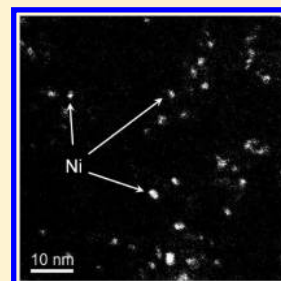
[⊥]Department of Chemistry, Middle East Technical University, Ankara, Turkey 06531

[#]Hungkuang University, Taichung, Taiwan 433

[¶]Shell Oil Company, Houston, Texas 77082, United States

S Supporting Information

ABSTRACT: Ziegler-type hydrogenation catalysts are important for industrial processes, namely, the large-scale selective hydrogenation of styrenic block copolymers. Ziegler-type hydrogenation catalysts are composed of a group 8–10 transition metal precatalyst plus an alkylaluminum cocatalyst (and they are not the same as Ziegler–Natta polymerization catalysts). However, for ~50 years two unsettled issues central to Ziegler-type hydrogenation catalysis are the nature of the metal species present after catalyst synthesis, and whether the species primarily responsible for catalytic hydrogenation activity are homogeneous (e.g., monometallic complexes) or heterogeneous (e.g., Ziegler nanoclusters defined as metal nanoclusters made from combination of Ziegler-type hydrogenation catalyst precursors). A critical review of the existing literature (Alley et al. *J. Mol. Catal. A: Chem.* **2010**, *315*, 1–27) and a recently published study using an Ir model system (Alley et al. *Inorg. Chem.* **2010**, *49*, 8131–8147) help to guide the present investigation of Ziegler-type hydrogenation catalysts made from the industrially favored precursors Co(neodecanoate)₂ or Ni(2-ethylhexanoate)₂, plus AlEt₃. The approach and methods used herein parallel those used in the study of the Ir model system. Specifically, a combination of Z-contrast scanning transmission electron microscopy (STEM), matrix assisted laser desorption ionization mass spectrometry (MALDI MS), and X-ray absorption fine structure (XAFS) spectroscopy are used to characterize the transition metal species both before and after hydrogenation. Kinetic studies including Hg(0) poisoning experiments are utilized to test which species are the most active catalysts. The main findings are that, both before and after catalytic cyclohexene hydrogenation, the species present comprise a broad distribution of metal cluster sizes from subnanometer to nanometer scale particles, with estimated mean cluster diameters of about 1 nm for both Co and Ni. The XAFS results also imply that the catalyst solutions are a mixture of the metal clusters described above, plus unreduced metal ions. The kinetics-based Hg(0) poisoning evidence suggests that Co and Ni Ziegler nanoclusters (i.e., M_{≥4}) are the most active Ziegler-type hydrogenation catalysts in these industrial systems. Overall, the novelty and primary conclusions of this study are as follows: (i) this study examines Co- and Ni-based catalysts made from the *actual industrial* precursor materials, catalysts that are notoriously problematic regarding their characterization; (ii) the Z-contrast STEM results reported herein represent, to our knowledge, the best microscopic analysis of the industrial Co and Ni Ziegler-type hydrogenation catalysts; (iii) this study is the first explicit application of an established method, using multiple analytical methods and kinetics-based studies, for distinguishing homogeneous from heterogeneous catalysis in these Ziegler-type systems; and (iv) this study parallels the successful study of an Ir model Ziegler catalyst system, thereby benefiting from a comparison to those previously unavailable findings, although the greater M–M bond energy, and tendency to agglomerate, of Ir versus Ni or Co are important differences to be noted. Overall, the main result of this work is that it provides the leading hypothesis going forward to try to refute in future work, namely, that sub, M_{≥4} to larger, M_n Ziegler nanoclusters are the dominant, industrial, Co- and Ni- plus AlR₃ catalysts in Ziegler-type hydrogenation systems.



INTRODUCTION

Ziegler-type hydrogenation catalysts are, by definition, formed from a non-zerovalent group 8–10 transition metal (M)

Received: January 5, 2011

Revised: March 11, 2011

Published: April 11, 2011

precatalyst such as Co(neodecanoate)₂ or Ni(2-ethylhexanoate)₂ plus a trialkylaluminum cocatalyst such as triethylaluminum (AlEt₃). Ziegler-type hydrogenation catalysts should not be confused, however, with Ziegler–Natta or other common polymerization catalysts, which are not a subject of this study. The relatively inexpensive Co- or Ni-based catalysts made from Co(neodecanoate)₂ or Ni(2-ethylhexanoate)₂, respectively, are significant industrially, as they are used in the production of $\sim 1.7 \times 10^5$ metric tons of hydrogenated styrenic block copolymers per year.¹ Several important fundamental questions about Ziegler-type hydrogenation catalysts persist despite the use of these catalysts for five decades.^{1–3} One of the most important remaining questions is the ~ 50 -year-old problem of whether the true nature of Ziegler-type hydrogenation catalysis is homogeneous (e.g., single metal organometallic) versus heterogeneous (e.g., nanoclusters).^{1,3–6}

A recently published critical review of Ziegler-type hydrogenation catalysts includes an examination of the prior evidence concerning their homogeneous versus heterogeneous nature. That review reveals that the reasons for the longevity of this problem, in this class of catalysts, include their sensitivity to variables and conditions in their preparation and use, plus their resistance to characterization by physical methods and isolation for kinetic studies.^{2,3} The literature review³ led to the suggestion that answering the homogeneous versus heterogeneous catalysis question for Ziegler-type hydrogenation catalysts could be facilitated through the use of a well characterized, third-row transition-metal precatalyst in combination with a multipronged, previously successful approach to solving the homogeneous versus heterogeneous catalysis problem in a variety of other catalyst systems.^{3,6–15} The central concepts of this multipronged approach toward answering the homogeneous versus heterogeneous catalysis question are (i) identification of the potential catalyst species using multiple complementary techniques, and then (ii) kinetic studies to determine the catalytic competency of those species.

Such studies using a Ziegler-type hydrogenation catalyst made from the crystallographically characterized precatalyst, [(1,5-COD)Ir(μ -O₂C₈H₁₅)₂], plus AlEt₃ have been recently published.¹⁴ Among the multiple analytical methods used were Z-contrast scanning transmission electron microscopy (STEM), matrix assisted laser desorption ionization mass spectrometry (MALDI MS), and X-ray absorption fine structure (XAFS) spectroscopy.¹⁴ Since “catalysis is, by definition, a wholly kinetic phenomenon”,¹⁶ kinetic studies were performed as a necessary component of addressing the homogeneous versus heterogeneous catalysis question.^{3,14} Those studies revealed that the Ir species present are different before versus after their use for catalytic cyclohexene hydrogenation. Specifically, before hydrogenation the catalyst solutions contain a wide range of Ir species from mono-Ir complexes up to structurally disordered Ir_{~100} Ziegler nanoclusters, with an estimated mean of 0.5–0.7 nm, Ir_{~4–15} clusters,¹⁴ whereas after hydrogenation, the Ir is in the form of fcc Ir(0)_{~40–150} Ziegler nanoclusters.¹⁴ Moreover, poisoning and other kinetic studies suggested that the fcc Ir(0)_{~40–150} Ziegler nanoclusters are the kinetically dominant catalysts.¹⁴

The goal of the present study is to repeat the analyses performed on the Ir model Ziegler-type hydrogenation catalyst system with Co- and Ni-based catalysts made from the authentic Co(neodecanoate)₂ or Ni(2-ethylhexanoate)₂ precursor materials used for industrial polymer hydrogenation. As such, this work

expands not only on our own previous study using the Ir model system,¹⁴ but also on the results of others—notably the valuable studies by Schmidt and co-workers,¹⁷ and Bönemann and co-workers¹⁸—that suggest transition metal nanoclusters are present in the Ziegler-type systems they studied.

Our main hypotheses for the present work are (i) that the approach that proved useful with the homogeneous vs heterogeneous catalysis question in the Ir system¹⁴ will be applicable to the industrial Co- and Ni-based systems, and (ii) that the results will be similar in that the most active catalysts will be revealed to consist of Co or Ni Ziegler nanoclusters, even if as small as Co₄ or Ni₄, that is subnanometer clusters. Many of the same analytical techniques are employed herein, namely, Z-contrast STEM, MALDI MS, XAFS spectroscopy (through its two complementary modifications, X-ray absorption near edge structure, or XANES, and extended XAFS, or EXAFS), and Hg(0) poisoning kinetics studies. Analogous to the previous study on the Ir model system,¹⁴ the specific objectives entail (i) determining the nuclearity of the M_n species present initially (M is Co or Ni), (ii) establishing what M_n species are present directly after use of the catalysts for cyclohexene hydrogenation, and (iii) using Hg(0) poisoning as a kinetics-based test of the homogeneous vs heterogeneous nature of the active catalyst.³ The challenging, yet crucial, issues of the form(s) taken and role(s) played by the AlEt₃ component in Ziegler-type hydrogenation catalysts are currently being investigated, and will be reported elsewhere in due course.¹⁹

Before the use of catalyst solutions for cyclohexene hydrogenation, the Z-contrast STEM and MALDI MS results which follow reveal that M_n clusters with a wide range of sizes are obtained from combining Co(neodecanoate)₂ or Ni(2-ethylhexanoate)₂, and AlEt₃, and the average cluster sizes are between 0.9 and 1.4 nm in diameter. The results of the Z-contrast STEM herein are, to the best of our knowledge, the best existing microscopic analysis of *industrial* Co and Ni Ziegler-type hydrogenation catalysts. The XANES spectroscopy results suggest that a combination of nanoclusters and unreduced metal ions exists, with the ratio of the two phases depending, as one might expect,³ on the Al/M ratio. EXAFS spectroscopic analysis of both Co and Ni catalyst samples gives mean first-nearest-neighbor (1NN) coordination number (*N*) values for both metals in the 3–4 range. The most plausible, self-consistent interpretation of the evidence from multiple, complementary techniques is that the transition metal contents of the catalyst solutions are a combination of disordered nanoclusters and unreduced, monometallic species. In addition, Z-contrast STEM, MALDI MS, and XAFS all show that the transition metal species in catalyst solutions remain essentially unchanged by their use for cyclohexene hydrogenation. Furthermore, Hg(0) poisoning studies suggest that catalysis is heterogeneous (i.e., occurs via the observed subnanometer or nanoscale M_{~4–130} clusters). Noteworthy here is that, since control experiments (vide infra and in the Supporting Information) show that AlEt₃ is required to generate an active catalyst (that XANES shows is reduced from Co(II)), species like Co–Et that can β -hydrogen eliminate to ethylene plus Co–H, and thus plausible species such as hydridic Co₄H₄ subnanometer clusters, all become candidates for the true catalyst. Through the use of an established approach to distinguish homogeneous from heterogeneous catalysis,^{3,6–15} and with the additional advantage of now being able to compare the results to those from a parallel study of an Ir model system, this study provides the best current evidence suggesting catalysis by what appear to be Ziegler

nanoclusters (i.e., $M_{\geq 4}$) in Ziegler-type hydrogenation catalysts made from the *actual* industrial Co and Ni precatalyst materials.

EXPERIMENTAL SECTION

Materials and Instruments. Material sources used to prepare catalyst solutions were kept consistent in order to obtain reproducible results (*vide infra*). All materials were stored and handled under a N_2 atmosphere in a Vacuum Atmospheres drybox, unless stated otherwise. Drybox O_2 levels were continuously monitored via a Vacuum Atmospheres O_2 -level indicator and maintained at ≤ 5 ppm. Gastight syringes were used to carry out all solution measurements and additions done in the Finke group drybox at Colorado State University (CSU). Procedures used to control the amount of H_2O present were followed consistently to ensure reproducibility (*vide infra*); glassware was rinsed with nanopure water, dried overnight at $160^\circ C$, and cooled under a vacuum or N_2 atmosphere. Cyclohexane (Sigma-Aldrich, 99.5%, $H_2O < 0.001\%$) was kept over molecular sieves (Acros, 3 Å, activated by heating at $200^\circ C$ for 6 h under vacuum) for ≥ 2 days prior to use with the Co catalyst, but used as received with the Ni catalyst (*vide infra*). Cyclohexene (Aldrich, 99%) was distilled over Na under argon. Precatalysts were obtained from OM Group, Inc., (OMG) as solutions in mineral spirits, Co(neodecanoate)₂, 12% wt Co, and Ni(2-ethylhexanoate)₂, 8% wt Ni (product names: 12% Co ten-cem and 8% Ni hex-cem). These industrial precatalyst sources of Co(neodecanoate)₂·*a*RCO₂H·*b*H₂O or Ni(2-ethylhexanoate)₂·*c*RCO₂H·*d*H₂O (both from OMG) are neither relatively pure nor well-characterized structurally compared to the Ir model [(1,5-COD)Ir(2-ethylhexanoate)]₂ precatalyst, which was characterized via single crystal X-ray diffractometry and used as the pure crystalline starting material for the preparation of catalyst solutions.^{1,14} Hereafter, we will refer to these as simply Co(neodecanoate)₂ and Ni(2-ethylhexanoate)₂ (i.e., *a,b,c,d* = 0). Both were used after diluting with cyclohexane to 12.0 mM in [M] (molecular weights of Co(neodecanoate)₂ and Ni(2-ethylhexanoate)₂ for dilutions were assumed to be the corresponding *a,b,c,d* = 0 values of 401.5 g/mol and 345.1 g/mol, respectively). AlEt₃ (Strem Chemicals, 93%) was used as a solution in cyclohexane. Both Ar and H₂ gases were passed through moisture (Scott Specialty Gases) and oxygen traps (Trigon Technologies) prior to use. THAP (2',4',6'-trihydroxyacetophenone, Aldrich, 98%), used in the MALDI MS experiments as a matrix, was stored and used outside of the drybox, and applied as an aqueous solution.

Catalyst Solution Preparation and Catalytic Cyclohexene Hydrogenations. Previous investigation into both the existing literature,³ and the Ir model system¹⁴ have made it clear that Ziegler-type hydrogenation catalysts are sensitive to the conditions and procedures used in their synthesis. We therefore carried out a variety of initial control experiments—testing the effects of catalyst aging, the Al/M ratio, the volume and concentration of catalyst solution prepared, the amount of H_2O present, temperature, concentration of AlEt₃ used, and order and rate of precursor component combination—all with the goal of ensuring that the characterization results obtained herein would be both reproducible and representative of active Ziegler-type hydrogenation catalysts. The results from these control experiments are briefly summarized here and given in greater detail in the Supporting Information for the interested reader. One of the important findings from these control experiments is the presence of gas-to-solution mass transfer limitation (MTL) effects in our current hydrogenation apparatus, which limits the *measurable* hydrogenation uptake rate to the rate of H_2 gas transfer into solution where the catalytic reaction takes place.²⁰ However, we have used catalyst preparation methods and conditions for this study that (i) result in catalytic cyclohexene hydrogenation rates that are at least as rapid as we can observe due to the MTL effects present, (ii) are consistent with the most favorable methods and conditions described in the majority of the literature,³ and (iii) are similar to, or the same as,

those used for the model Ir Ziegler-type hydrogenation catalyst made from [(1,5-COD)Ir(μ -O₂C₈H₁₅)]₂ and AlEt₃.^{1,14} In short, the MTL kinetics present for these exceptionally active, industrial Ziegler-type hydrogenation catalysts did not preclude our determination of conditions and procedures for catalyst synthesis necessary to give results that are both reproducible and representative of active Ziegler-type hydrogenation catalysts standardized to the MTL limit of our apparatus.

Once established, the procedures for preparing and using catalyst solutions (referred to hereafter as the *standard conditions*) were followed consistently for repeat experiments unless specified otherwise. Control experiments demonstrate that the presence of (deliberately added) water during catalyst synthesis negatively affects the cyclohexene hydrogenation activity of the resulting catalysts. Therefore, all glassware was carefully dried as was the cyclohexane solvent for use with the Co-based catalyst (cyclohexane drying was not beneficial for the Ni catalysts; see the Supporting Information). The catalyst solutions were made under a N_2 atmosphere by combination of a 36.0 mM cyclohexane solution of AlEt₃ with a 12.0 mM Co(neodecanoate)₂ or Ni(2-ethylhexanoate)₂ precatalyst stock solution. The ratios Al/Co = 3 and Al/Ni = 2 were used for the standard conditions on the basis of control experiments testing catalysts prepared with a range of Al/M values. Control experiments were performed with an Al/M ratio of zero for both Co and Ni, and it was found that no H_2 gas uptake occurred without added AlEt₃, which shows the importance of the alkylaluminum cocatalyst in making active Ziegler-type hydrogenation catalysts.

Synthesis of catalyst solutions in batches up to 20 mL, as opposed to the 2.5 mL of catalyst solution prepared for use in a single hydrogenation run, had no observable effect on catalyst activity. Likewise, batch catalyst preparation at 7.2 mM in [M] had no observable effect on catalyst activity in comparison to the 1.44 mM in [M] catalyst solutions prepared for use in a single hydrogenation run (diluted after preparation to 1.2 mM in [M] with the addition of 0.5 mL of cyclohexene). Therefore, it was possible to prepare catalyst solutions either individually or batchwise as necessary, and at concentrations necessary for the subsequent type of analysis. Catalyst synthesis carried out with solutions heated to $60^\circ C$ resulted in catalyst solutions with lower cyclohexene hydrogenation activity (Supporting Information); hence, catalyst synthesis at the ambient drybox temperature of $\sim 25^\circ C$ was established as a standard condition. For the sake of consistency, and unless noted otherwise, catalyst solutions were prepared by adding the AlEt₃ solution to either the Co(neodecanoate)₂ or Ni(2-ethylhexanoate)₂ solution dropwise but rapidly (at a rate ≥ 1 drop every 5 s), and with 1000 \pm 200 rpm stirring (measured with a Monarch Instruments Pocket-Tachometer 100). As an example of batch catalyst preparation, 20 mL of catalyst solution was prepared by first adding 16.8 mL of cyclohexane to a 20 mL glass vial containing a new 5/8 \times 5/16 in Teflon-coated magnetic stir bar. Next, 1.6 mL of a 12.0 mM cyclohexane solution of Ni(2-ethylhexanoate)₂ was added. Stirring was started, followed by addition of 1.6 mL of a 36.0 mM AlEt₃ solution. Stirring in the drybox was continued for 30 min, after which aliquots of the catalyst solution were taken for analysis or transferred to a new 22 \times 175 mm Pyrex borosilicate culture tube containing a new 5/8 \times 5/16 in Teflon-coated magnetic stir bar for kinetic studies via use in cyclohexene hydrogenation. Since, as noted above, volume and concentration had no effect on hydrogenation, catalyst solutions were also prepared directly in the culture tubes for individual hydrogenation runs by, for example, first adding 1.9 mL of cyclohexane to a culture tube followed by 0.3 mL of a cyclohexane solution of Co(neodecanoate)₂, 12.0 mM in [Co]. Stirring was started and then 0.3 mL of the 36.0 mM AlEt₃ solution in cyclohexane was added. Cyclohexene, 0.5 mL, was added last. In general, the procedures used in this study were very similar to, and in a number of cases the same as, those used previously for the Ir model system.¹⁴

After combination of the precursor components, cyclohexene was added to catalyst solutions used for catalytic hydrogenation runs.

Control experiments show that aging prepared catalyst solutions resulted in *decreased* catalyst activity (Supporting Information), so catalysts were used for hydrogenation or otherwise analyzed as soon as possible after preparation. The procedure and apparatus used for catalytic cyclohexene hydrogenation have been described in detail elsewhere.²¹ Briefly, the culture tube containing the catalyst solution was placed in a Fisher-Porter (F–P) bottle, sealed, and transferred out of the drybox. The F–P bottle was placed in a temperature regulating bath, stirring was begun, and the F–P bottle was connected to a pressurized H₂ line using Swagelock quick-connects. The F–P bottle was purged 15 times (1 purge/15 s) before setting the pressure to 40 psig. Data collection was then started at 4 min after the first purge. H₂ pressure data as a function of time were collected using an Omega PX 624–100 GSV pressure transducer, which was connected to a PC running *LabView 7.0* by an Omega D1131 analog-to-digital converter. Data were subsequently handled using *MS Excel* and *Origin 7*. Standard conditions for hydrogenation runs are as follows: solvent = cyclohexane, [M] = 1.2 mM, initial [cyclohexene] = 1.65 M, temp = 22.0 °C, initial H₂ pressure = 40 psig, and stirring rate = 1000 ± 10 rpm. The main point is that, in both catalyst synthesis and subsequent hydrogenations, variables with the potential to influence the resulting catalytic activity have been tested and optimized (to the MTL limit), thereby allowing the development of standard conditions for the preparation and use of the highly active Ziegler-type hydrogenation catalysts used herein. This in turn ensures that the subsequent analytical results should be both reproducible and representative of active Ziegler-type hydrogenation catalysts.

Z-Contrast STEM. Catalyst samples were prepared according to standard conditions as described; they were then collected for Z-contrast microscopy both before and after use in cyclohexene hydrogenation. Sample solutions were double-sealed airtight, and shipped to the University of Pittsburgh for imaging (2–3 days between preparation and analysis). Preparation of samples on TEM grids was carried out in a glovebag filled with dry N₂ at >1 atm, and located in the TEM room. Sample solutions were diluted with cyclohexane to twice their original volume, and 2–3 drops were dispersed onto a TEM grid with an ultrathin carbon film on a holey carbon support (Ted Pella, Inc.). These were dried at room temperature under N₂ for ≥ 10 min before being transferred into the TEM instrument. Transfer was done quickly to reduce possible oxidation of the sample. Samples were first treated with a high-intensity electron beam (electron beam shower) for ~15 min each time in the TEM column (with vacuum better than 3 × 10⁻⁶ Torr). Images were acquired using a field-emission JEM 2010 (scanning) transmission electron microscope operated at 200 kV. The high-angle scattering electrons were collected with a JEOL ADF detector at a camera length of 8 cm, with a 0.2 nm (nominal) diameter probe. High-angle annular dark-field (HAADF) images were collected at 2 M (million) magnification, and were 1024 × 1024 pixels in dimension. Cluster diameters were measured manually at the full width at half-maximum (fwhm) of the intensity profile across ≥ 600 clusters from images at the same levels of magnification and contrast using Gatan Digital Micrograph.

Control experiments were performed to determine whether the metal clusters observed were artifacts of the microscopy itself. Co(neodecanoate)₂, without added AlEt₃, was deposited on a TEM grid (ultrathin carbon film supported by a lacey carbon film on a 400 Mesh copper grid, Ted Pella), and imaged following the methods noted above (i.e., including the electron beam shower). No Co clusters could be observed, suggesting that neither the sample preparation procedures, nor the Z-contrast STEM conditions, are responsible for creating the observed clusters in catalyst samples. No Co clusters were observed when this same control experiment was carried out using high resolution (HR)TEM. (The fact that Co in Co(neodecanoate)₂ could not be observed in Z-contrast STEM images *without* Co cluster formation has a bearing on the interpretation of the EXAFS results, *vide infra*; specifically, it leaves open the possibility that monometallic, unreduced metal

ions are present.) Additionally, Co(neodecanoate)₂, without added AlEt₃, was deposited on special TEM grids with 25-nm-thick SiO₂ windows (Dune Sciences).²² However, for this sample on the special SiO₂ grids, imaging using bright field TEM, Z-contrast STEM, and HRTEM all revealed the presence of nanometer-scale clusters, ostensibly the result of Co cluster formation under the TEM beam. These control experiments suggest that the clusters observed using Z-contrast STEM imaging of catalyst samples deposited on ultrathin carbon grids, and resultant cluster size histograms, are not artifacts resulting from the required sample handling or microscopy itself. Images from control experiments and additional microscopy are provided in the Supporting Information for the interested reader.

MALDI MS. Catalyst samples were prepared for analysis by MALDI MS in a manner almost identical to that described previously using the Ir model system.¹⁴ A 0.5 μL, 100 mM aqueous NaI ionizing agent solution was hand-spotted on a steel MS sample plate and air-dried, which was followed by 1 μL of 2',4',6'-trihydroxyacetophenone (THAP) over the same spot and then also air-dried. The plate was then transferred into the drybox where sample solutions (1 μL, [M] = 1.44 mM) were applied onto the spot of deposited ionizing agent and matrix. The plate was then covered with its plastic capping plate and placed into a desiccator, which was sealed and removed from the drybox. The plate was transferred in air (exposure of ~30 s) from the desiccator to the vacuum of the MALDI MS instrument, and MALDI MS spectra were taken immediately thereafter. Mass spectra were obtained at CSU on a Bruker Ultraflex TOF-TOF instrument in linear mode, with acceleration voltage at 25 kV, and in positive ion mode. A nitrogen laser (λ = 337 nm) with a 3 ns pulse width was focused over a 1-mm-diameter spot. Data were collected with the highest laser power possible, for a higher S/N, but which still maximized resolution and avoided sample fragmentation. Calibration was done using Bradykinin, Angiotensin_I, Angiotensin_II, Substance_P, Bombesin, Renin_Substrate, ACTH_clip and Somatostatin (purchased as a mixture of all these peptides from Bruker-Daltonics).

XAFS. Procedures for XAFS spectroscopy herein are similar to those used previously for the analysis of the Ir model system.¹⁴ Solution samples of Co(neodecanoate)₂, Ni(2-ethylhexanoate)₂, and catalysts made from these plus AlEt₃ were prepared at Colorado State University, in 6.0 mL batches at 7.2 mM concentration in [M]. Aliquots of catalyst samples were used for cyclohexene hydrogenation in order to obtain both pre- and posthydrogenation catalyst samples. All samples were then sealed airtight, and transported to the National Synchrotron Light Source (NSLS) at Brookhaven National Laboratory (BNL), Upton, NY (2 days transit). At the NSLS, catalyst samples were handled and stored in an N₂ atmosphere glovebox maintained at ≤ 10 ppm O₂. Catalyst samples were loaded, via glass pipet, into a custom-designed, airtight, ~1.5 mL capacity, solution sample cell composed of a stainless steel frame made to press Kapton film windows onto a Teflon block. Threaded ports in the Teflon block allow for sample loading, which were then sealed using Teflon screws. Airtight seals in the threaded ports and windows were ensured by using Kalrez o-rings. XAFS experiments were performed at room temperature on beamline X18b or X11a, which are sourced by bending magnets, and employ Si(111) double-crystal monochromators. Samples were loaded into an airtight sample cell, then mounted and positioned at 45° in the beam path. Three 30-cm-long ion chambers filled with suitable gas mixtures were employed to record in transmission mode the incident, transmitted, and reference beam. A Lytle detector was used to measure fluorescence data simultaneously with transmission, but the fluorescence spectra were deemed of inferior quality to the transmission spectra and, therefore, not used in the analysis. Co or Ni foils were used both for absorption edge calibration of the Co (7709 eV) and Ni (8333 eV) K edges prior to XAFS scans. Co and Ni foils were also used to obtain reference spectra simultaneously in transmission mode for all sample scans. Six to eight scans were typically performed for each sample; during data processing multiple scans of a single sample were merged (averaged).

Data processing was accomplished using IFEFFIT.²³ For background removal, threshold energy values (E_0) for both Co and Ni were assigned values corresponding to the inflection point in the normalized absorption edges. A Hanning window function was used to select data ranges in k -space with sufficient signal-to-noise ratio for Fourier transforms (FTs) (Supporting Information). The passive electron reduction factors (S_0^2) for Co and Ni were acquired from fitting the Co and Ni foil standards, respectively (Supporting Information). Parameters including the coordination numbers (N), bond lengths (R), and their disorders (σ^2) were varied in the fitting of catalyst sample spectra, as well as the correction to the photoelectron energy origin (ΔE_0). Details of fitting EXAFS spectra are given in the Supporting Information.

Hg(0) Poisoning. Catalyst solutions for use in Hg(0) poisoning experiments were first prepared in the drybox according to the standard conditions as described with $[M]$ concentration of 1.2 mM (M is Co or Ni), an Al/Co ratio of 3.0, or an Al/Ni ratio of 2.0, and initial cyclohexene concentrations of 1.65 M. In one version of the Hg(0) poisoning experiment, a standard conditions hydrogenation was stopped after about half the cyclohexene had been consumed by filling and purging the F–P bottle five times with Ar gas pressurized to 40 psig. The F–P bottle was then transferred back into the drybox where the Hg(0) was added and allowed to mix for the specified time (24 h for Co, 1.5 h for Ni). The F–P bottle was then reconnected to the hydrogenation line, refilled with H_2 gas using the standard procedure and data acquisition was restarted. Time and pressure values collected after Hg(0) addition were corrected to fit with the data collected before Hg(0) addition (see Figure 10). In another version of the Hg(0) poisoning experiment, Hg(0) was added to the catalyst solutions before cyclohexene hydrogenation catalysis was started and allowed to mix for the specified time. The bottle containing the catalyst solution and Hg(0) was then transferred to the pressurized H_2 to collect pressure data using normal procedures.

The results of Hg(0) poisoning control experiments are shown in the Supporting Information for the interested reader. In the case of the Co catalyst, eight control experiments carried out independently by two different researchers (WMA and KHY) using ~ 1700 equiv of Hg(0) per Co and 24 h of mixing show that the degree of poisoning of the Co catalyst when Hg(0) is added prior to the start of cyclohexene hydrogenation is irreproducible. For the Ni catalyst, control experiments using various quantities of Hg(0) added to prepared catalyst solutions, followed by various mixing times before their use in hydrogenation, show that a procedure using ≥ 300 equiv of Hg(0) per Ni and ≥ 1.5 h of stirring (at 1000 rpm in a sealed FP bottle in the drybox) is adequate to thoroughly contact the Hg(0) with all of the Ni catalyst in solution; this procedure was then strictly followed and proved reproducible. Other control experiments show that both the Co and Ni catalyst solutions retain catalytic activity when subjected to the handling procedures required for Hg(0) addition, but in the absence of Hg(0). Restated, those additional controls show that it is the Hg(0) itself, and not the procedures, that poison the catalysis (see the Supporting Information for details).

RESULTS AND DISCUSSION

Initial Observations, Plus an Overview of the Key Pre- and Posthydrogenation Characterization Results. As noted in a review of the literature of the homogeneous versus heterogeneous catalysis problem,⁶ initial observations of the catalyst solutions alone make industrial Ziegler-type catalysts candidates for study regarding the homogeneous vs heterogeneous catalysis question. Specifically, dark brown or black solutions are frequently observed in literature catalyst systems now known to involve heterogeneous (e.g., nanoparticle) catalysis, making such an observation, by itself, *suggestive* of heterogeneous catalysis.⁶ In

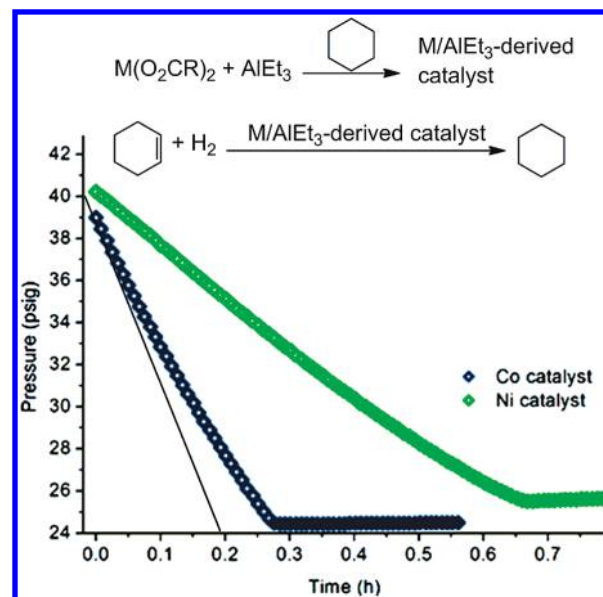


Figure 1. Top: general steps for the synthesis of Co- or Ni-based Ziegler-type hydrogenation catalyst solutions; $M(O_2CR)_2$ is either of the authentic industrial precatalysts, $Co(neodecanoate)_2$ or $Ni(2\text{-ethylhexanoate})_2$. Catalyst solutions were made by combining a cyclohexane solution of one of the precatalysts, 12.0 mM in $[M]$, with a 36.0 mM cyclohexane solution of $AlEt_3$. Example catalytic cyclohexene hydrogenation curves using standard conditions of solvent = cyclohexane, $[M] = 1.2$ mM, initial $[cyclohexene] = 1.65$ M, temp = 22.0 °C, and stirring rate = 1000 ± 10 rpm are shown. The apparent MTL value, depicted here as a black line, is $\sim 80 \pm 20$ psig/h in our apparatus and at these conditions (e.g., at the 1000 ± 10 rpm stirring rate).

the present study, there are several noteworthy observations from the synthesis of the industrial Co- and Ni-based catalysts, especially in comparison with the observations from the Ir model system.¹⁴ For example, addition of the clear and colorless solution of $AlEt_3$ to the clear, deep-blue $Co(neodecanoate)_2$ solution results in an immediate change to a *dark brown, almost black solution*. Likewise, addition of the $AlEt_3$ solution to the clear, light-green solution of $Ni(2\text{-ethylhexanoate})_2$ causes an immediate change to a *dark brown solution* (but one that is a lighter shade of brown than the $Co/AlEt_3$ catalyst solution). Unlike with the $[(1,5\text{-COD})Ir(\mu\text{-}O_2C_8H_{15})_2]_2$ plus $AlEt_3$ catalyst system, which is a much lighter, yellow-brown solution after addition of $AlEt_3$ but darkens during a cyclohexene hydrogenation run, and will occasionally precipitate a dark-brown powder a few days after the completion of a hydrogenation run,¹⁴ these industrial Co- or Ni-based catalysts do not exhibit observable color change or insoluble particle formation during, or post, hydrogenation. Using the Ir model catalyst, it was found that H_2 uptake begins initially at a slower rate, then accelerates to achieve its maximum rate after the start of hydrogenation (i.e., the initial rate is not the maximum rate).¹⁴ Furthermore, this increase in cyclohexene hydrogenation rate during the hydrogenation using the model Ir catalyst is accompanied by the observation of, on average, $Ir_{\sim 4-15}$ clusters prehydrogenation, but $fcc\ Ir(0)_{\sim 40-150}$ clusters posthydrogenation.

In contrast, with the industrial Co- or Ni-based catalysts, H_2 uptake begins immediately at the apparent H_2 gas-to-solution MTL rate ($\sim 80 \pm 20$ psig/h at 1000 rpm stirring; Supporting Information) or at $\sim 30\%$ of the apparent H_2 gas-to-solution MTL rate, respectively (Figure 1). This implies that, in the

Table 1. Summary of Results from Investigation of Metal Cluster Sizes Using Z-Contrast STEM and MALDI MS for Industrial Ziegler-Type Hydrogenation Catalysts Made from Co(neodecanoate)₂ or Ni(2-ethylhexanoate)₂ plus AlEt₃ (Al/Co is 3.0, Al/Ni is 2.0), and for Comparison an Ir Ziegler-Type Hydrogenation Catalyst made from [(1,5-COD)Ir(μ -O₂C₈H₁₅)₂] plus AlEt₃ (Al/Ir is 2.0), Both before and after Use for Cyclohexene Hydrogenation

	analytical method	precatalysis			postcatalysis		
		range (nm)	average ^a (nm)	average ^a M _n nuclearity	range (nm)	average ^a (nm)	average ^a M _n nuclearity
Co	Z-contrast STEM	0.6–3.3	1.4	Co _{~130}	0.5–2.5	1.4	Co _{~130}
	MALDI MS	0.8–1.8	1.2	Co _{~80}	0.8–1.8	1.1	Co _{~60}
Ni	Z-contrast STEM	0.4–3.5	1.3	Ni _{~100}	0.6–4.0	1.4	Ni _{~130}
	MALDI MS	0.8–1.7	0.9	Ni _{~34}	0.8–1.6	0.9	Ni _{~34}
Ir ^b	Z-contrast STEM	0.2–1.4	0.5	Ir _{~4}	0.4–1.9	1.0	Ir _{~40}
	MALDI MS	0.5–1.1	0.7	Ir _{~15}	0.6–1.4	0.8	Ir _{~20}

^aThe average values are calculated mean cluster diameters from Z-contrast STEM, and estimated mean nuclearities from MALDI MS. Explanations for how these values were determined, and how the cluster diameter-nuclearity conversion is performed, are given below. ^bResults from a previously published study,¹⁴ provided here for comparison.

industrial Co- or Ni-based catalysts, very active catalyst species are present initially after the addition of AlEt₃, or possibly are formed essentially immediately upon the introduction of H₂ gas. In short, the initial observations from catalyst preparation alone are consistent with the presence of Co and Ni Ziegler nanoclusters in catalyst solutions both initially and throughout the hydrogenation process.

These initial observations of the dark colors of the catalyst solutions explain why the specific objectives herein necessarily entail (i) determining the nuclearity of the M_n species present *initially*, and (ii) establishing what M_n species are present *directly after* use of the catalysts for cyclohexene hydrogenation. These are the necessary first steps in probing the homogeneous versus heterogeneous nature of the most active catalyst in these industrial systems.

A summary of the results obtained from the analysis of catalyst samples pre- and posthydrogenation by Z-contrast STEM and MALDI MS is given in Table 1 alongside the results from the Ir model system for comparison.¹⁴ The key findings for both the Co- and Ni-based catalysts are the following: (i) Z-contrast STEM and MALDI MS reveal nanometer-scale clusters for both Co and Ni samples, both before and after hydrogenation; and (ii) the XAFS data indicate that unreduced metal ions are present in solution, depending on the Al/M ratio, with the nanometer-scale Co_n or Ni_n clusters present. In addition, the XAFS shows those Co_n and Ni_n clusters possess disordered atomic structures. In short, disordered transition metal Ziegler nanoclusters appear to be the predominant clusters formed by the industrial Co- and Ni-based precatalysts upon addition of AlEt₃, both before and after hydrogenation, yet monometallic (homogeneous) species appear to be present as well. In addition, the ability to directly compare the results obtained herein to the results from the prior, analogous study of the model Ir system,¹⁴ is a valuable, unique feature of the present study.

Nuclearity of M_n Species before Hydrogenation: Z-Contrast STEM. Samples of the Co(neodecanoate)₂ plus AlEt₃ catalyst, with an Al/Co ratio of 3.0, *before* use for cyclohexene hydrogenation were imaged using Z-contrast STEM. Measurement of 604 clusters shows a range of Co cluster sizes from 0.6 to 3.3 nm in diameter, with a mode and median of 1.3 nm clusters, and a mean Co cluster diameter of 1.4 ± 0.4 nm. These cluster diameters correspond to cluster nuclearities with a range from Co_{~10} to Co_{~1700}, a mode and median of Co_{~100},

and a mean of Co_{~130}.^{24–26} Figure 2 shows an example image and the histogram.

Samples of the Ni(2-ethylhexanoate)₂ plus AlEt₃ catalyst, with an Al/Ni ratio of 2.0, *before* use for cyclohexene hydrogenation were also imaged using Z-contrast STEM. An example image and the histogram are shown in Figure 3. Measurement of 650 clusters in Z-contrast STEM images reveals a range of Ni cluster sizes from 0.4 to 3.5 nm in diameter. The mode, median, and mean Ni cluster diameters are 1.1 nm, 1.2 nm, and 1.3 ± 0.5 nm, respectively. These diameters correspond to cluster nuclearities ranging from Ni_{~3} to Ni_{~2050}, the mode, median, and mean being Ni_{~60}, Ni_{~80}, and Ni_{~100}, respectively.^{24–26}

For both Co and Ni samples, Z-contrast STEM shows the presence of metal clusters with a broad distribution of sizes ranging from subnanometer to several nanometers in diameter. Cluster diameter measurements were made using the full width at half-maximum (fwhm) of line intensity profiles across individual clusters. These Z-contrast microscopy results by themselves should not be considered absolutely definitive, however, due to the possibility that the observed clusters could be artifacts of the microscopy itself, especially given that lighter (first-row) transition metal clusters and precursors are known to be less stable in TEM electron beams than their heavier (third-row) analogs—a key reason we began our studies with our now-published third-row metal, Ir-model system.^{14,27–29} More specifically, Ni Ziegler-type hydrogenation catalysts have been observed to be sensitive to electron microscopy sample treatment processes, specifically, drying of the Ni catalyst solution on TEM grids.² However, the possibility of artifactual results is mitigated herein by the use of *scanning* TEM,³⁰ which diminishes the potential for beam-induced sample damage via a small electron probe, low beam current, and minimal beam exposure time.³¹ The images herein were watched during image acquisition for signs of the influence of the TEM beam on the catalyst sample, and no changes in cluster size or shape were observed. In addition, control experiments (described in the Experimental Section, images shown in the Supporting Information) suggest that the clusters observed using Z-contrast STEM, and measured to construct the cluster size histograms, are not artifacts. To summarize, Z-contrast microscopy shows that Co and Ni catalyst samples, *before* hydrogenation, each contain a wide range of M_n clusters, 1.4 ± 0.4 nm, Co_{~130}, and 1.3 ± 0.5 nm, Ni_{~100}, being the mean cluster size and nuclearity in each case, respectively. To the extent

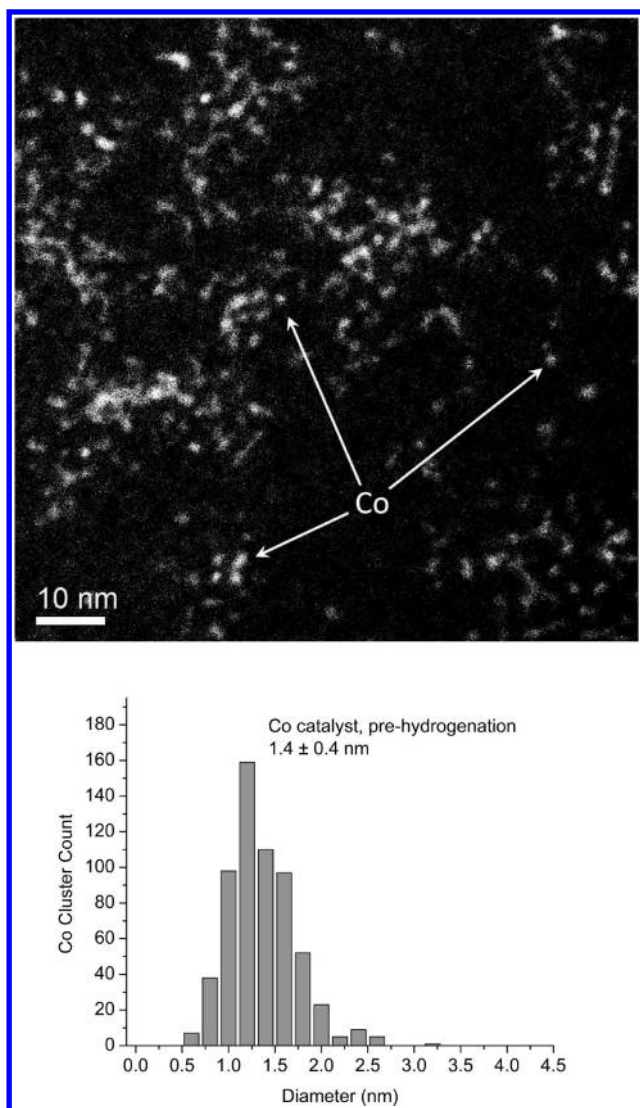


Figure 2. Example Z-contrast STEM image of the $\text{Co}(\text{neodecanoate})_2$ plus AlEt_3 catalyst, with an Al/Co ratio of 3.0, and before its use for cyclohexene hydrogenation. The histogram from measuring 604 Co clusters reveals an overall range of Co clusters observed from 0.6 to 3.3 nm in diameter, which correspond to $\text{Co}_{\sim 10}$ to $\text{Co}_{\sim 1700}$ clusters. The Co clusters measured have a mode and median of 1.3 nm, and a mean diameter of 1.4 ± 0.4 , corresponding to $\text{Co}_{\sim 100}$ and $\text{Co}_{\sim 130}$ clusters, respectively.^{24–26}

of our knowledge, the results of the Z-contrast STEM herein are the best existing microscopic analysis of *industrial* Co and Ni Ziegler-type hydrogenation catalysts.

Nuclearity of M_n Species before Hydrogenation: MALDI MS. Samples of the $\text{Co}(\text{neodecanoate})_2$ plus AlEt_3 catalyst, with an Al/Co ratio of 3.0, were also analyzed using MALDI MS before their use in cyclohexene hydrogenation. A broad peak is observed with a maximum intensity at ~ 4500 m/z (figures are shown in the Supporting Information). With the assumptions that the ions forming the broad peaks are composed of only Co atoms,^{32–34} and that the ionic charge is $+1$,^{14,32,34,35} the maximum intensity of the MALDI MS peak at ~ 4500 m/z corresponds to $\text{Co}_{\sim 80}$ clusters. This, in turn, corresponds to a diameter approaching ~ 1.2 nm (used as an estimate of the average Co clusters reported in Table 1). Furthermore, the broad

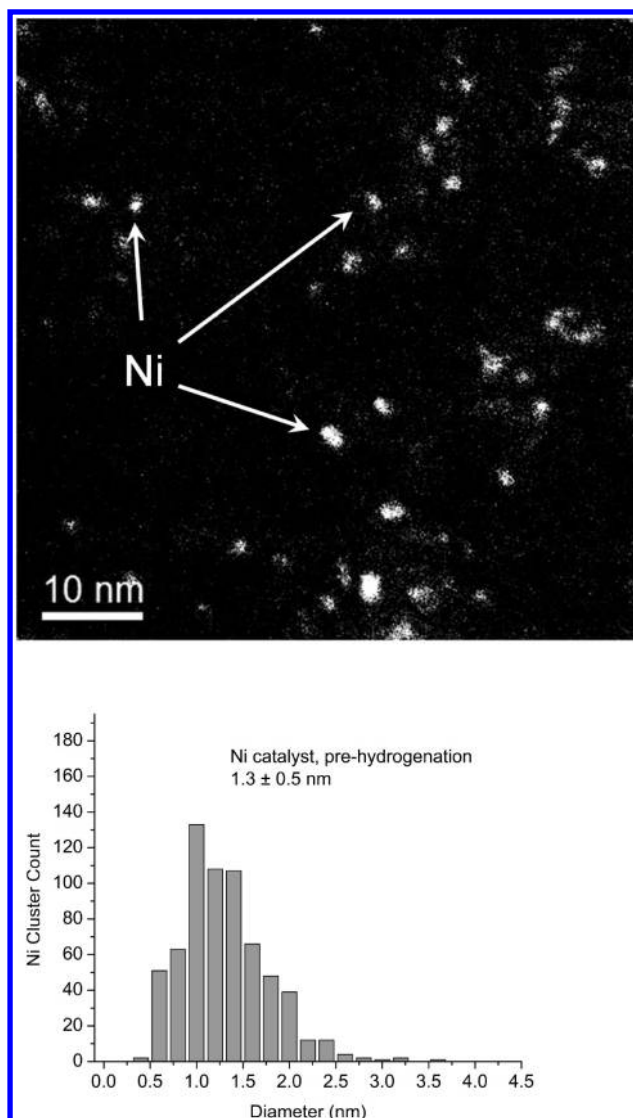


Figure 3. Example Z-contrast STEM image of the $\text{Ni}(\text{2-ethylhexanoate})_2$ plus AlEt_3 catalyst with an Al/Ni ratio of 2.0, and before use for cyclohexene hydrogenation. The histogram made from measurement of 650 Ni clusters shows Ni cluster sizes ranging from 0.4 to 3.5 nm in diameter, which correspond to $\text{Ni}_{\sim 3}$ to $\text{Ni}_{\sim 2050}$ clusters. The Ni clusters measured have a mode of 1.1 nm, a median of 1.2 nm, and a mean diameter of 1.3 ± 0.5 nm, corresponding to $\text{Ni}_{\sim 60}$, $\text{Ni}_{\sim 80}$, and $\text{Ni}_{\sim 100}$, respectively.^{24–26}

MALDI MS peak also indicates a wide size dispersity of the Co clusters present, similar to the wide size dispersity of the Co clusters observed using Z-contrast STEM. The fwhm of the broad, asymmetrically shaped MALDI MS peak is from ~ 2000 – 9000 m/z , and tails off toward higher m/z values. The peak reaches one-fourth maximum intensity at ~ 12000 m/z and one-eighth maximum intensity at ~ 16000 m/z ; these m/z values correspond to approximately $\text{Co}_{\sim 30-150}$, $\text{Co}_{\sim 200}$, and $\text{Co}_{\sim 270}$ clusters, respectively, which in turn correspond to approximately 0.9–1.5, 1.6, and 1.8 nm Co clusters, respectively.

Samples of the $\text{Ni}(\text{2-ethylhexanoate})_2$ plus AlEt_3 catalyst, with an Al/Ni ratio of 2.0, were also analyzed using MALDI MS before their use in cyclohexene hydrogenation. A broad peak is observed with a maximum intensity at m/z of 2000. However, the presence

of Ni atoms in species below 1500 m/z is ruled out by the absence of characteristic Ni isotope peak distributions in that region. In a control experiment, the MALDI MS of a blank sample containing only the matrix, trihydroxyacetophenone (THAP), and ionizing agent, NaI, contains peaks in the 0–1500 m/z range (Supporting Information). Therefore, the 0–1500 m/z range was excluded from the mass spectrum region used to calculate number of transition metal atoms (M) in the M_n clusters and corresponding diameters, for both Co and Ni catalyst samples; the m/z values of 1500–16 000 for Co and 1500–13 500 for Ni were used to calculate the cluster diameter ranges reported in Table 1. Using the same assumptions employed for the Co system above, as well as previously in the literature,^{14,32–35} the maximum intensity of the broad peak at m/z of ~ 2000 indicates $Ni_{\sim 34}$ clusters, corresponding to ~ 0.9 -nm-diameter Ni nanoclusters (used as an estimate of the average Ni clusters reported in Table 1). Much like the MALDI MS peak of the Co catalyst (and of the Ir model system¹⁴), the broad, asymmetrically shaped peak of the Ni catalyst also tails off toward higher m/z values reaching ~ 6000 m/z at half-maximum intensity, ~ 9000 m/z at one-fourth maximum intensity, and $\sim 13\,500$ m/z at one-eighth maximum intensity, which correspond to approximately $Ni_{\sim 100}$, $Ni_{\sim 150}$, and $Ni_{\sim 230}$, respectively. These nuclearities correspond, in turn, to approximately 1.3, 1.5, and 1.7 nm Ni nanoclusters, respectively.

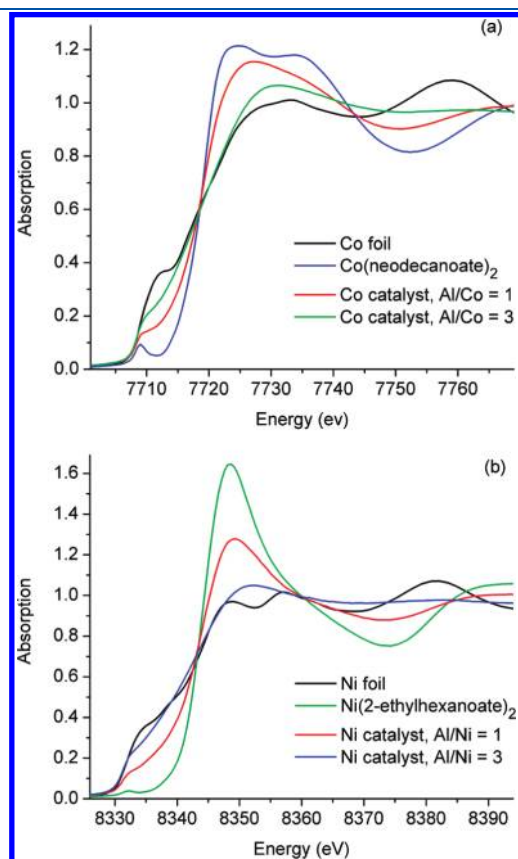


Figure 4. (a) XANES spectra of Co foil (black) the Co(neodecanoate)₂ catalyst precursor without added AlEt₃ (blue), and Co(neodecanoate)₂ plus AlEt₃ catalysts with Al/Co ratios of 1.0 (red) and 3.0 (green). (b) XANES spectra of Ni foil (black), the Ni(2-ethylhexanoate)₂ catalyst precursor without added AlEt₃ (green), and Ni(2-ethylhexanoate)₂ plus AlEt₃ catalysts with Al/Ni ratios of 1.0 (pink) and 3.0 (blue). In each case, with additional AlEt₃, the XANES spectra of the catalyst solution becomes less like the precursor solution and more like the metal foil.

Somewhat as an aside, this study, and the previous one of the Ir model system,¹⁴ are interesting, if not unique tests of the value of MALDI MS as an analytical method for measuring the size and size distribution of transition metal nanoclusters since they obtain MALDI MS data on systems where Z-contrast STEM (and XAFS, *vide infra*) data are available for comparison. Overall, the MALDI MS-estimated nanocluster sizes and size distributions for both Co and Ni prehydrogenation catalysts are generally consistent with those determined using Z-contrast STEM in showing cluster sizes in the ranges 0.8–1.8 nm for Co and 0.8–1.7 nm for Ni are present.

Nuclearity of M_n Species before Hydrogenation: XAFS (i.e., XANES plus EXAFS) Spectroscopy. The XANES spectra of both Co and Ni catalysts are compared to those of the corresponding metal foils and catalyst precursors in Figure 4. In each case, the XANES spectra of the catalyst solution become less like that of the precursor solution and more like that of the metal foil with higher Al/M ratios. This suggests that, in terms of composite average formal oxidation state, the Co or Ni metals in catalyst solutions become progressively less like their M(II) precatalysts and progressively more similar to M(0), as the Al/M ratios increase from 1.0 to 3.0. These results imply that unreduced metal ions are likely present in catalyst solutions in amounts that decrease with additional AlEt₃. Given the M_n nanoclusters observed using both Z-contrast STEM and MALDI MS, these results suggest that catalyst solutions contain a combination of M_n clusters with a wide range of diameters and unreduced metal ions, with the proportion of M atoms in the cluster versus ion phases depending on the Al/M ratio used in catalyst preparation.

The potential of EXAFS spectroscopy for the characterization of Ziegler-type hydrogenation catalysts, especially the industrially favored Co and Ni catalysts, was made apparent to us by the valuable prior studies of Goulon and co-workers.³⁶ Specifically, those authors found Ni–Ni first nearest neighbors indicating the presence of Ni metal clusters.³⁶ However, additional study proved worthwhile using modern EXAFS analysis methods that use *ab initio* theory for the quantitative modeling and analysis of experimental EXAFS spectra,³⁷ especially when considered alongside results of complementary Z-contrast STEM and MALDI MS techniques used herein, the Hg(0) poisoning studies, and the now-possible comparison to the results obtained from the Ir model system.¹⁴

First, EXAFS data were collected separately for Co and Ni foils, and cyclohexane solutions of the Co(neodecanoate)₂ and Ni(2-ethylhexanoate)₂ precatalysts, without added AlEt₃, for use as reference samples (see Supporting Information for the full results, including fits to the data). Solution samples of the catalysts prepared by addition of AlEt₃, but before their use in cyclohexene hydrogenation, were then analyzed by EXAFS. Spectra were collected for catalyst samples with Al/M ratios of 0.5, 1.0, 1.5, 2.0, 2.5, 3.0, and 5.0. However, the EXAFS spectra of many of these samples were of sufficiently poor quality to make fitting and interpretation unreliable. The highest quality spectra were obtained for the Al/M = 1.0 and 3.0 samples; therefore, the spectra and fitting results of the Al/M = 1.0 and 3.0 samples are shown here, but the spectra and fitting results from samples prepared at other Al/M ratios are shown in the Supporting Information.³⁸ For both Co and Ni catalysts, sample spectra show peaks that correspond to the first nearest neighbor (1NN) M–O peak in the precatalyst spectra, and to the first nearest neighbor (1NN) M–M peak in the M foil spectra, Figure 5. This is analogous to the catalyst spectra of the Ir model catalyst

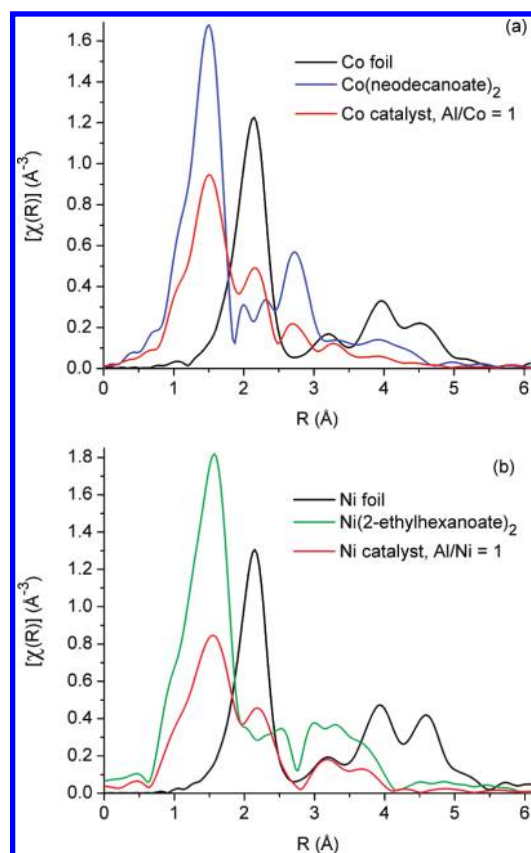


Figure 5. (a) Fourier transform magnitudes of the k^2 -weighted EXAFS spectra of Co metal foil (black), the $\text{Co}(\text{neodecanoate})_2$ pre-catalyst without added AlEt_3 (blue), and a sample of the $\text{Co}(\text{neodecanoate})_2$ plus AlEt_3 catalyst with an Al/Co ratio of 1.0 before its use for hydrogenation (red). (b) Fourier transform magnitudes of the k^2 -weighted EXAFS spectra of Ni foil (black), the $\text{Ni}(\text{2-ethylhexanoate})_2$ pre-catalyst without added AlEt_3 (green), and a sample of the $\text{Ni}(\text{2-ethylhexanoate})_2$ plus AlEt_3 catalyst with an Al/Ni ratio of 1.0 before its use for hydrogenation (pink). Upon addition of AlEt_3 , the Co and Ni catalyst samples still show a peak corresponding to the 1NN, M–O peak of the $\text{Co}(\text{neodecanoate})_2$ and $\text{Ni}(\text{2-ethylhexanoate})_2$ pre-catalysts, respectively, but also display a peak corresponding to the 1NN, M–M peak from the spectrum of the bulk metal. Also, and significantly, catalyst samples lack peaks in the 3–6 Å range characteristic of ordered, metallic structure. Spectra for Co and Ni foils are shown at one-fourth intensity scale for the purpose of comparison.

system;¹⁴ hence, the fitting strategy used herein for the Co- or Ni-based catalysts is analogous to the one employed to fit the EXAFS spectra of the Ir model catalyst samples.¹⁴ The Co and Ni catalyst spectra were fit using composite models created from the 1NN M–O path of the pre-catalyst and the 1NN M–M path of the bulk metal. Examples of fitting results are shown in Figure 6, and given in Tables 2 and 3.

The main results from EXAFS are as follows: (i) peaks in the 3–6 Å range in the R -space EXAFS spectra (indicative of ordered metallic structures and evident in the Co and Ni foil reference spectra, Figure 5) are absent for both Co and Ni catalyst samples. The lack of the large distance peaks observed here suggests that Co and Ni catalyst samples are (a) composed of metal species such as subnanometer metal clusters too small to have contributions in that interatomic distance range, (b) are composed of larger metal nanoclusters with a high degree of atomic disorder,

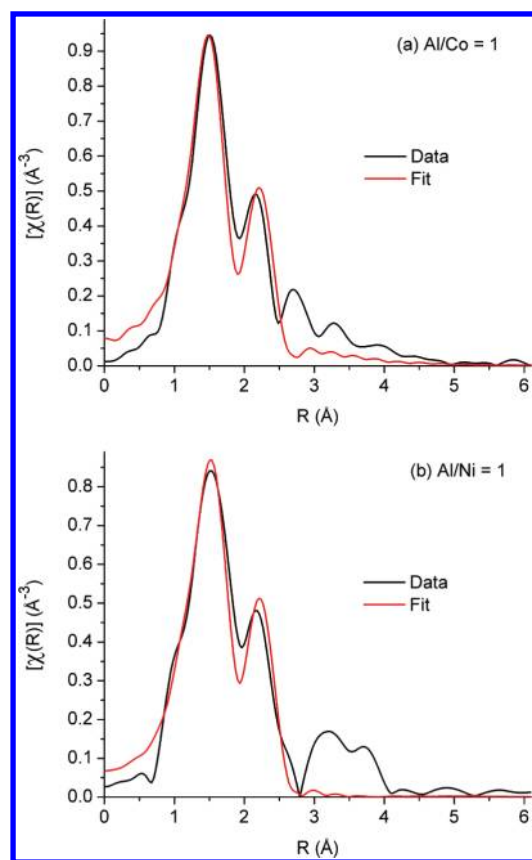


Figure 6. Data and fits for (a) $\text{Co}(\text{neodecanoate})_2$ plus AlEt_3 catalyst and (b) $\text{Ni}(\text{2-ethylhexanoate})_2$ plus AlEt_3 catalyst, with an Al/M ratio of 1.0 in each case. The highest quality spectra were obtained for the Al/M = 1.0 and 3.0 samples; the experimental spectra and fits to the Al/M = 1.0 data are shown here as examples—spectra and fitting results from samples prepared at other Al/M ratios are shown in the Supporting Information.

Table 2. Fitting Results from EXAFS Spectroscopic Analysis of Co Reference Samples and $\text{Co}(\text{neodecanoate})_2$ plus AlEt_3 Catalyst Samples before Hydrogenation

Sample	Al/Co	Co foil	$\text{Co}(\text{O}_2\text{CR})_2^a$	Co catalyst 1.0	Co catalyst 3.0
$N_{\text{Co-Co}}$		12^d		3 ± 2	3.9 ± 0.4
$N_{\text{Co-O}}$			4.7 ± 0.4	3.5 ± 0.9	3 ± 2
$R_{\text{Co-Co}} (\text{Å})^b$		2.492 ± 0.002		2.51 ± 0.02	2.432 ± 0.009
$R_{\text{Co-O}} (\text{Å})^b$			1.959 ± 0.005	1.95 ± 0.02	1.86 ± 0.02
$\sigma^2_{\text{Co-Co}} (\text{Å}^2)^c$		6.7 ± 0.3		15 ± 6	12 ± 1
$\sigma^2_{\text{Co-O}} (\text{Å}^2)^c$			4.6 ± 0.7	7 ± 3	20 ± 7

^a $\text{Co}(\text{O}_2\text{CR})_2$ is the catalyst precursor $\text{Co}(\text{neodecanoate})_2$ without added AlEt_3 . The full analysis of $\text{Co}(\text{neodecanoate})_2$ is given in the Supporting Information. ^b R stands for the interatomic distance corresponding to the single scattering paths. ^c σ^2 represents the mean square variation in R due to both static and dynamic disorder (also known as the EXAFS Debye–Waller factor), and values shown are $\times 10^3$. ^d For Co foil, this parameter was defined as the value shown (i.e., not varied in the fit).

or (c) are some combination of the two. The next main result from the EXAFS data is that (ii) spectra are fit reasonably well using a composite model generally analogous to the one employed for the Ir model system.¹⁴ Significantly, and unlike in the Ir

Table 3. Fitting Results from EXAFS Spectroscopic Analysis of Ni Reference Samples and Ni(2-ethylhexanoate)₂ plus AlEt₃ Catalyst Samples before Hydrogenation

Sample	Al/Ni	Ni foil	Ni(O ₂ CR) ₂ ^a	Ni catalyst 1.0	Ni catalyst 3.0
N _{Ni–Ni}		12 ^d		3 ± 1	4.4 ± 0.3
N _{Ni–O}			5.8 ± 0.3	2.8 ± 0.5	1.2 ± 0.3
R _{Ni–Ni} (Å) ^b	2.490 ± 0.003			2.51 ± 0.02	2.447 ± 0.006
R _{Ni–O} (Å) ^b			2.035 ± 0.005	2.00 ± 0.02	1.85 ± 0.01
σ ² _{Ni–Ni} (Å ²) ^c	6.9 ± 0.5			13 ± 4	12.4 ± 0.8
σ ² _{Ni–O} (Å ²) ^c			7.4 ± 0.7	8 ± 3	14 ± 5

^aNi(O₂CR)₂ is the catalyst precursor Ni(2-ethylhexanoate)₂ without added AlEt₃. The full analysis of Ni(2-ethylhexanoate)₂ is given in the Supporting Information. ^bR stands for the interatomic distance corresponding to the single scattering paths. ^cσ² represents the mean square variation in R due to both static and dynamic disorder (also known as the EXAFS Debye–Waller factor), and values shown are × 10³. ^dFor Ni foil, this parameter was defined as the value shown (i.e., not varied in the fit).

model system however, the catalyst samples with an Al/M ratio of 3.0 did not require incorporating a backscattering contribution from M–Al into the model, although a reasonable possibility here is that the quality (or, the signal-to-noise) of the Co and Ni EXAFS data is insufficient to distinguish a M–Al feature. Furthermore, the spectra themselves (Figure 6) lack the feature observed in the spectra of the Ir model system that “grew in” with successively greater Al/M ratios. From fitting the data, (iii) the 1NN M–M coordination numbers observed for Co and Ni samples are, like those observed in the Ir model system studied previously,¹⁴ roughly in the 3–4 range, and could point toward the predominance of, on average, subnanometer, M_{~4–6}, metal clusters in catalyst solutions before hydrogenation.³⁹ Alternatively, low 1NN M–M coordination numbers could signify a large degree of structural disorder in relatively large metal nanoclusters.^{14,40} The σ²_{M–M} values of the catalyst samples are approximately twice the experimentally determined bulk metal values (Tables 2 and 3), which is also suggestive of disordered nanoclusters. Another possibility is that the metal species in catalyst solutions exist as some combination of disordered clusters and unreduced metal ions.

An additional main result from EXAFS is that (iv) the closest M–M distances, given by 1NN R_{M–M} values, overlap within experimental error with the corresponding bulk metals for both Co and Ni samples with Al/M ratios of 1.0, but for Al/M = 3.0 are shorter than the bulk metal M–M distances. M–M distances in nanometer scale metal particles with a bulk-like atomic structure are expected to be shorter on average than the corresponding bulk M–M distances due to M–M bond contraction required to counteract (i.e., decrease)^{40a–d,41} the high surface free energy of the small metal clusters. Therefore, the implication is that the Co or Ni catalyst materials are becoming structurally more like nanoscale metal particles with increasing amounts of AlEt₃, but not to the point that the 1NN N_{M–M} values increase significantly or long-range metallic order becomes apparent in the 3–6 Å range in the R-space EXAFS spectra (which is also consistent with the changes in the XANES spectra given above).

Interpretation of the EXAFS results from the Co and Ni samples must be carried out in light of the Z-contrast STEM, MALDI MS, and XANES results. For example, the 1NN N_{M–M} values from EXAFS of roughly 3–4 seem, at first take, to imply, on average, M_{~4–6} clusters analogous to the Ir results. However,

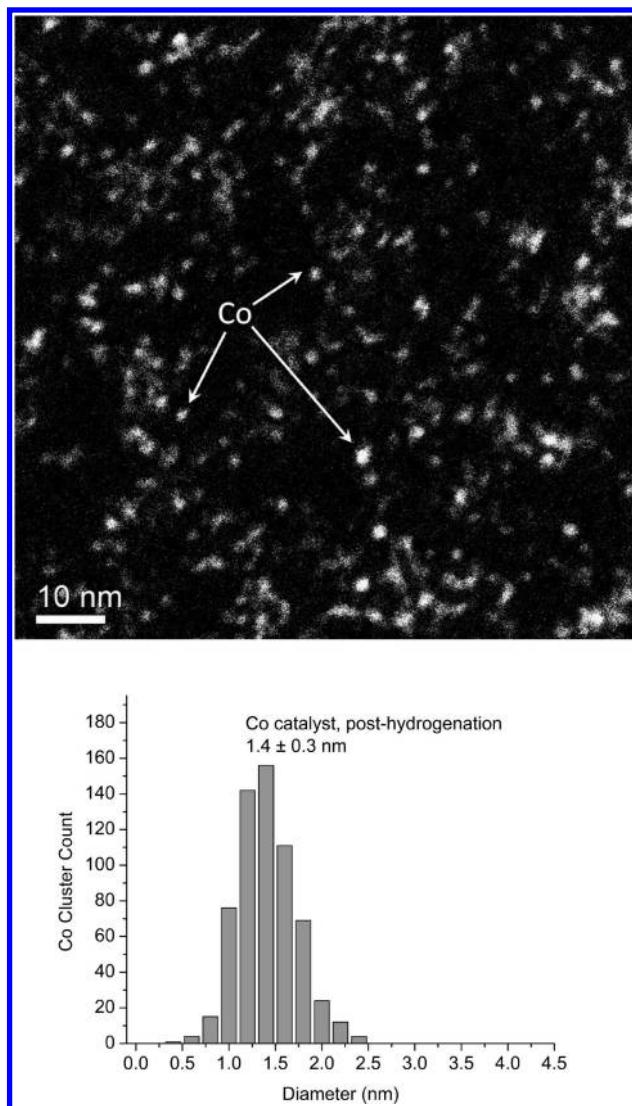


Figure 7. Example Z-contrast STEM image of a Co(neodecanoate)₂ plus AlEt₃ catalyst sample, Al/Co = 3.0, after its use in hydrogenation. The histogram shows the results from measuring the diameters of 614 Co clusters in such images; measured cluster diameters range from 0.5 to 2.5 nm, which correspond to Co cluster nuclearities from Co_{~6} to Co_{~740}. The mode, median, and mean diameters of Co clusters are 1.3, 1.4, and 1.4 ± 0.3 nm, corresponding to Co_{~100} or Co_{~130} accordingly.

the Z-contrast STEM reveals mean Co or Ni cluster diameters of 1.4 or 1.3 nm, respectively, that is, M_{~130} to M_{~100} clusters. Therefore, the most plausible explanation for the results from combining the Z-contrast STEM, MALDI MS, and XAFS (i.e., XANES and EXAFS) spectroscopy appears to be that a combination of nanoclusters (which are structurally disordered resulting in the absence of peaks at larger distances in the R-space EXAFS spectra and distorted 1NN N_{M–M} values from fits of the EXAFS spectra⁴²) and unreduced metal ions are present, with these two phases of M species both contributing to the mean N_{M–M} value.^{40i,43} The possibility of monometallic, unreduced metal ions being present is supported by the control experiments for Z-contrast STEM in which no Co was observable when only Co(neodecanoate)₂, without AlEt₃, was on the sample grid. In other words, the metal-containing species in Co and Ni catalyst solutions appear to consist of disordered metal clusters with a

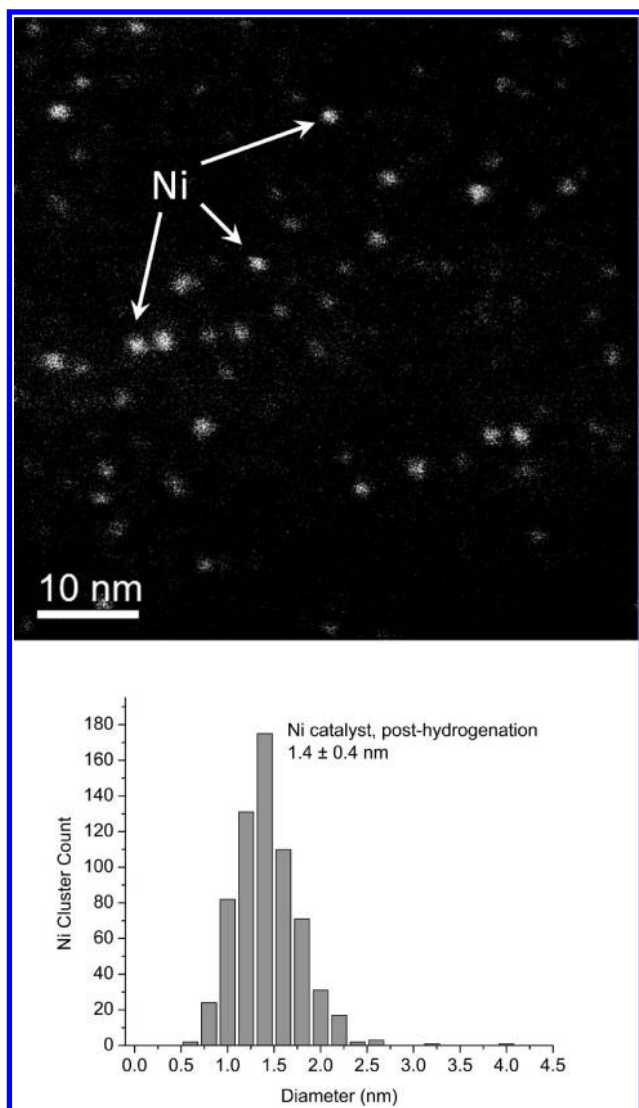


Figure 8. Example Z-contrast STEM image of a Ni(2-ethylhexanoate)₂ plus AlEt₃ catalyst sample, Al/Ni = 2.0, after its use in hydrogenation. The corresponding histogram shows the results from measuring the diameters of 650 Ni clusters in such images, and reveals a range of Ni clusters with diameters from 0.6 to 4.0 nm, corresponding to Ni_{~10} to Ni_{~3060}. The mode and median diameters are 1.4 nm, and the mean is 1.4 ± 0.4 nm, corresponding to mean Ni_{~130} clusters.

broad distribution of sizes, the mean diameters of which are given by Z-contrast STEM and MALDI MS, plus some monometallic complexes present as unreduced metal ionic species. Noteworthy here is that it is the industrial Co and Ni catalysts, and Al/M ratios and conditions, that have been examined, to which these conclusions refer.

Nuclearity of M_n Species after Hydrogenation: Z-contrast STEM. The Co(neodecanoate)₂ plus AlEt₃ catalyst, with an Al/Co ratio of 3.0, and after its use for cyclohexene hydrogenation was imaged using Z-contrast STEM. Measurement of 614 clusters shows a range of Co cluster sizes 0.5–2.5 nm in diameter. The mode, median, and mean Co cluster diameters are 1.3, 1.4, and 1.4 ± 0.3 nm, corresponding to Co_{~100} and Co_{~130}, accordingly. Figure 7 shows an example image and the histogram.

The Ni(2-ethylhexanoate)₂ plus AlEt₃ catalyst, with an Al/Ni ratio of 2.0, after its use for cyclohexene hydrogenation was also imaged using Z-contrast STEM. Measurement of 650 clusters in Z-contrast STEM images reveals a range of Ni cluster sizes 0.6–4.0 nm in diameter. The mode and median Ni cluster diameter is 1.4 nm and the mean is 1.4 ± 0.4 nm. These diameters correspond to Ni_{~130}. An example image and the histogram are shown in Figure 8.

Z-contrast STEM shows that using these Co and Ni Ziegler-type hydrogenation catalysts for cyclohexene hydrogenation does not induce a change in the sizes of the metal cluster species present in either Co or Ni catalyst samples, at least under the conditions used herein. Although this differs from the distinct increase in metal cluster size and change in structure exhibited by the Ir model system,¹⁴ it is consistent with the lack of changes in catalyst solution color, no observation of precipitates in post-hydrogenation solutions (unlike the Ir model system¹⁴). In short, catalytic cyclohexene hydrogenation induces essentially no changes in size or size distribution of the Co or Ni clusters observed by Z-contrast STEM.

Nuclearity of M_n Species after Hydrogenation: MALDI MS. Samples of the Co(neodecanoate)₂ plus AlEt₃ catalyst, with an Al/Co ratio of 3.0, were analyzed using MALDI MS after their use in cyclohexene hydrogenation (figures are shown in the Supporting Information). MALDI MS of the Co catalyst results in a broad peak with maximum intensity at ~3500 *m/z* (reported as the average Co cluster in Table 1) and a shoulder at ~6000 *m/z*. Using the same necessary assumptions as before, that the broad peaks are composed of only +1 charged ions,^{14,32–35} the peak at ~3500 *m/z* indicates Co_{~60} clusters, corresponding to a diameter of ~1.1 nm. The peak of the posthydrogenation Co catalyst tails off toward higher *m/z* values; fwhm of the peak is from ~1500–9500 *m/z*, the peak reaches one-fourth maximum intensity at ~12 000 *m/z*, and one-eighth maximum intensity at ~17 000 *m/z* (1500–17 000 is used to report the range of Co clusters in Table 1), which correspond to 0.8–1.5 nm, Co_{~25–160}; 1.6 nm, Co_{~200}; and 1.8 nm, Co_{~290} clusters, respectively—essentially the same as the prehydrogenation results.

The Ni(2-ethylhexanoate)₂ plus AlEt₃ catalyst, with an Al/Ni ratio of 2.0, was also analyzed using MALDI MS after it had been used for cyclohexene hydrogenation, giving a broad peak with a maximum intensity at ~2000 *m/z*, which again indicates Ni_{~34} clusters, corresponding to ~0.9-nm-diameter Ni nanoclusters (reported as the average cluster size in Table 1). (As in the catalyst sample before hydrogenation, the presence of Ni atoms in species below 1500 *m/z* is ruled out by the absence of characteristic Ni isotope peak distributions in that region.) The broad, asymmetrically shaped MALDI MS peak of the catalyst sample after hydrogenation also tails off toward higher *m/z* values, but is not completely identical to the peak of the sample before hydrogenation; the posthydrogenation peak displays two slight shoulders at ~3000 and ~6000 *m/z*. Nevertheless, the broad peak in the sample after hydrogenation reaches ~6500 *m/z* at half-maximum intensity, ~8500 *m/z* at one-fourth maximum intensity, and ~11 000 *m/z* at one-eighth maximum intensity (1500–11 000 *m/z* is used to report the range of Ni clusters in Table 1), which correspond to 1.3 nm, Ni_{~110}; 1.5 nm, Ni_{~145}; and 1.6 nm, Ni_{~190}, respectively. These Ni cluster size and nuclearity values are very similar to those from the prehydrogenation sample. In short, the MALDI MS-determined sizes and size distributions of both Co and Ni clusters in posthydrogenation

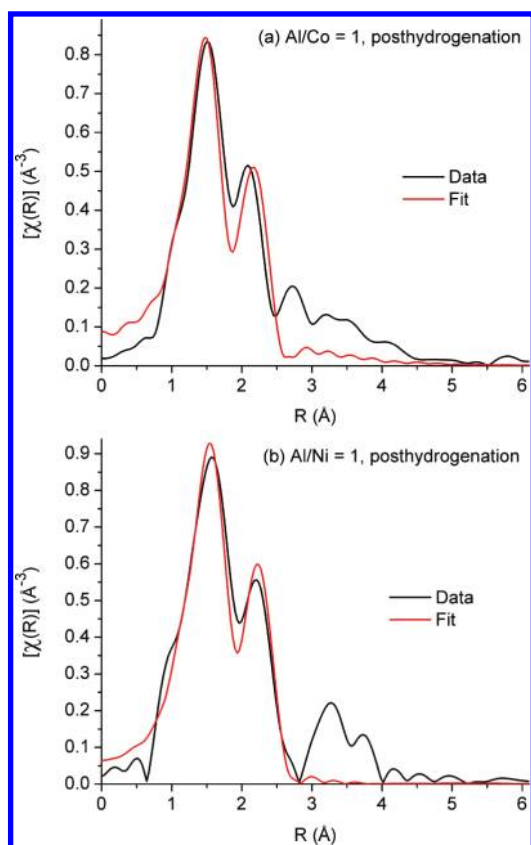


Figure 9. Data and fits of (a) the $\text{Co}(\text{neodecanoate})_2$ plus AlEt_3 catalyst, Al/Co ratio of 1.0; and (b) the $\text{Ni}(\text{2-ethylhexanoate})_2$ plus AlEt_3 catalyst, Al/Ni ratio of 1.0; both after use of the catalytic hydrogenation of cyclohexene. The R-ranges used for the fits of these samples are 1.0–2.8 Å and 1.0–2.6 Å for Co and Ni, respectively.

samples (i) agree closely with the analysis of posthydrogenation catalyst samples using Z-contrast STEM, are consistent with the Z-contrast STEM, and (ii) indicate no significant change in the sizes of the metal clusters present upon their use for the catalytic hydrogenation of cyclohexene.

Nuclearity of M_n Species after Hydrogenation: XAFS (i.e., XANES and EXAFS) Spectroscopy. Solution samples of both $\text{Co}(\text{neodecanoate})_2$ plus AlEt_3 and $\text{Ni}(\text{2-ethylhexanoate})_2$ plus AlEt_3 catalysts, with Al/M ratios of 1.0, were analyzed using XAFS after their use in hydrogenation reactions. The XANES spectra of the Co and Ni catalyst solutions posthydrogenation are nearly the same as their prehydrogenation counterparts. XANES spectra collected after hydrogenation are shown and compared to the prehydrogenation spectra in the Supporting Information for the interested reader. For both Co and Ni catalysts, the EXAFS spectra after hydrogenation also appear very similar to the sample spectra before hydrogenation. The spectra are fit using the same models employed for fitting the catalyst samples before hydrogenation. The results are shown in Figure 9 and summarized in Table 4. Complete fit information and additional spectra are in the Supporting Information.

The most plausible interpretation of the EXAFS spectra and fitting results is essentially the same for the catalyst samples after hydrogenation as for the samples before hydrogenation. The lack of peaks in the 3–6 Å range corresponding to the peaks observed in this range for Co and Ni bulk metals implies that no Co or Ni species with ordered metallic structures on that scale are present,

Table 4. Summary of Fit Results for Posthydrogenation Co and Ni Catalyst Spectra

Sample	Co	Ni
N_{M-M}	3 ± 2	3 ± 1
N_{M-O}	3 ± 1	2.7 ± 0.4
R_{M-M} (Å) ^a	2.48 ± 0.02	2.52 ± 0.01
R_{M-O} (Å) ^a	1.96 ± 0.02	2.02 ± 0.01
σ^2_{M-M} (Å ²) ^b	15 ± 7	13 ± 3
σ^2_{M-O} (Å ²) ^b	7 ± 4	7 ± 2

^a R stands for the interatomic distance corresponding to the single scattering paths. ^b σ^2 represents the mean square variation in R due to both static and dynamic disorder (the EXAFS Debye–Waller factor), and values shown are $\times 10^3$.

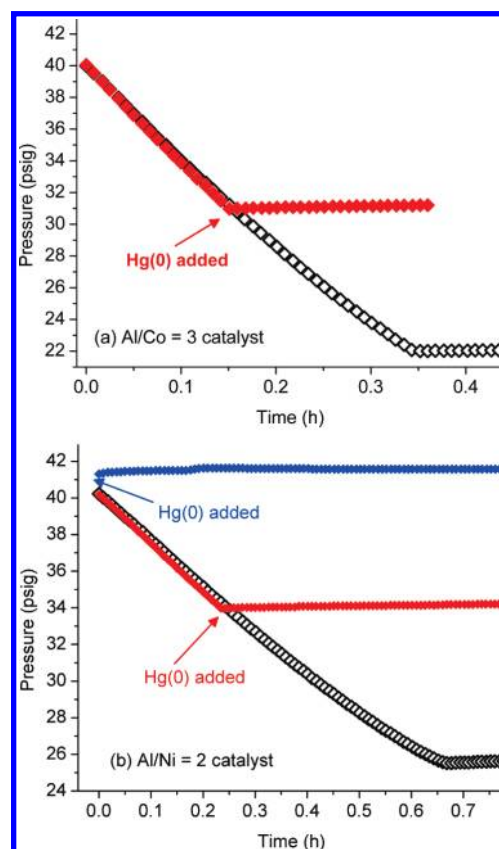


Figure 10. Poisoning experiments using the $\text{Co}(\text{neodecanoate})_2$ or $\text{Ni}(\text{2-ethylhexanoate})_2$ plus AlEt_3 catalysts, with an Al/Co ratio of 3.0 or an Al/Ni ratio of 2.0, are shown next to standard example cyclohexene hydrogenation runs for comparison (black curves). (a) For the Co catalyst, an example poisoning experiment shows immediate and complete poisoning of catalysis by $\text{Hg}(0)$ addition partway through a cyclohexene hydrogenation run (red curve). This result was reproducible (3 trials). (b) For the Ni catalyst, immediate and complete poisoning of catalysis is observed upon addition of $\text{Hg}(0)$ both partway through a catalytic run (red), and after preparation of the catalyst but before hydrogenation is begun (blue). These results suggest that catalysis in the industrial Co and Ni Ziegler-type hydrogenation systems is heterogeneous (i.e., via the observed M_n nanoclusters, $n \geq 4$).

and 1NN single scattering N_{M-M} values of ~ 3 were obtained for both Co and Ni catalysts. Additionally, the R_{M-M} values from both Co and Ni samples posthydrogenation are the same as their

prehydrogenation counterparts within experimental error, and are very close to the experimental bulk metal values (within ≤ 0.03 Å). Recall from the discussion of the prehydrogenation XAFS results that bulk metal-like R_{M-M} values are in contrast to the larger R_{M-M} values expected for subnanometer M_n clusters ligated by Lewis acid species (i.e., $AlEt_3$ and its derivatives). Lastly, the σ^2_{M-M} values of the catalyst samples are again roughly twice the experimentally determined bulk metal values. Considered in light of the posthydrogenation Z-contrast and MALDI MS results, which reveal a predominance of nanometer scale clusters as part of wide size distributions, the self-consistent interpretation of all measurements (made already for the prehydrogenation samples) is that a combination of disordered nanoclusters and unreduced, monometallic species are present in catalyst solutions posthydrogenation. In short, both the XANES and EXAFS spectra confirm that use of catalyst solutions for cyclohexene hydrogenation has a negligible effect on the oxidation state and form of the transition metal catalyst material.

Kinetics Studies: Hg(0) Catalyst Poisoning. The observation of M_n clusters before and after catalysis does not necessitate that these species are the active hydrogenation catalysts—kinetic studies are required to determine the most active catalyst(s) from sample solutions. Catalyst poisoning by Hg(0) is a useful, kinetics-based test for distinguishing homogeneous from heterogeneous Ziegler-type hydrogenation catalysis, as has been shown previously.¹⁴ Hence, Hg(0) poisoning experiments were utilized to test whether the observed catalytic activity of the industrial Ziegler-type hydrogenation catalysts made from $Co(neodecanoate)_2$ or $Ni(2-ethylhexanoate)_2$ and $AlEt_3$ is “homogeneous” (e.g., via single metal organometallic) or “heterogeneous” (e.g., via small M_4 or larger nanoclusters) (Figure 10). One benefit of using Hg(0) poisoning in this case is that the results should be largely unaffected by MTL kinetics (vide supra, and in the Supporting Information).

Two different versions of the Hg(0) poisoning experiment were performed in order to emulate the study of the Ir system.¹⁴ In one version, the Hg(0) is added after about half the cyclohexene has been consumed. In the other version, the Hg(0) is added after the initial catalyst synthesis, prior to the start of cyclohexene hydrogenation (i.e., before the catalyst solution is placed under pressurized H_2). When Hg(0) is added to the Co catalyst solution after about half the cyclohexene has been consumed, the Hg(0) reproducibly poisons the catalysis *immediately and completely* (Figure 10a). However, when the Hg(0) is added after the initial Co catalyst synthesis, eight attempts using ~ 1700 equiv of Hg(0) per Co and 24 h of mixing, conducted separately by two different researchers, show that the extent of poisoning observed is irreproducible (Supporting Information).

In the case of the nickel catalyst, when Hg(0) is added to the Ni catalyst solution after about half the cyclohexene has been consumed, the Hg(0) reproducibly poisons the catalysis *immediately and completely* (Figure 10b). Unlike the observation with the Co catalyst, Hg(0) addition to the Ni catalyst prior to the start of cyclohexene hydrogenation also poisons catalysis *immediately, completely*, and reproducibly (Figure 10b).

An explanation for the irreproducibility observed when attempting to poison the Co catalyst prior to the start of cyclohexene hydrogenation is not immediately apparent. One possibility is that the active catalyst is changing rapidly at the start of cyclohexene hydrogenation from one that is not poisoned by Hg(0) (i.e., a homogeneous catalyst) to one that is poisoned by Hg(0) (i.e., a heterogeneous catalyst). However, this is merely

speculation; elucidation of the cause of the irreproducible poisoning would require additional investigation and an improved understanding of the fundamental interaction between Hg(0) and the Co species present. It is known that one potential difficulty with Hg(0) poisoning experiments is that it may be difficult to thoroughly contact the Hg(0) with all of the catalyst in solution due to the insolubility of Hg(0).⁴⁴ However, for the Ni system, control experiments allowed the determination that a procedure using ≥ 300 equiv of Hg(0) per Ni and ≥ 1.5 h of 1000 rpm stirring is adequate to thoroughly contact the Hg(0) with all of the Ni catalyst in solution. Nevertheless, and with the possible exceptions implied by the irreproducible results using the Co system, the Hg(0) poisoning results ultimately suggest that catalysis in the industrial Ziegler-type hydrogenation systems, made from $Co(neodecanoate)_2$ or $Ni(2-ethylhexanoate)_2$ precatalysts plus $AlEt_3$ are “heterogeneous”, that is, catalysis occurs via the observed sub, M_{4-6} to larger $M_{\sim 130}$ nanoclusters.

Conclusions and Needed Future Studies. Catalysts made from either of the industrial precursors $Co(neodecanoate)_2$ or $Ni(2-ethylhexanoate)_2$, plus $AlEt_3$, were analyzed by Z-contrast STEM, MALDI MS, XAFS (i.e., XANES and EXAFS), and Hg(0) poisoning studies, producing the following, key observations: (i) Co and Ni Ziegler-type hydrogenation catalyst solutions turn dark brown upon the initial combination of the $Co(neodecanoate)_2$ or $Ni(2-ethylhexanoate)_2$ precatalyst solutions with the $AlEt_3$ solution, and not during hydrogenation catalysis as observed with the Ir model system; and (ii) hydrogenation proceeds immediately with the start of data acquisition at, or very near, the maximum observable rate. (iii) Z-contrast STEM reveals, for the prehydrogenation Co sample, a 0.6–3.3 nm range of particle diameters with a mean of 1.4 ± 0.4 nm, which corresponds to $Co_{\sim 130}$. For the prehydrogenation Ni sample, Z-contrast STEM reveals a 0.4–3.5 nm range of particle diameters with a mean of 1.3 ± 0.5 nm, which corresponds to $Ni_{\sim 100}$. (iv) MALDI MS is used to estimate, for the prehydrogenation Co sample, a 0.8–1.8 nm range of particle diameters and an average of 1.2 nm, which corresponds to $Co_{\sim 80}$. For the prehydrogenation Ni sample, MALDI MS is used to estimate a 0.8–1.7 nm range of particle diameters and an average of 0.9 nm, which corresponds to $Ni_{\sim 34}$. (v) XANES spectra show that the Co or Ni metals in prehydrogenation catalyst solutions become progressively less like their M(II) precatalysts, in terms of composite average formal oxidation state, and progressively more like the M(0) metal foils as the Al/M ratios increase from 1.0 to 3.0, implying that unreduced metal ions are present in catalyst solutions in amounts that decrease with additional $AlEt_3$. (vi) EXAFS spectroscopic analysis of prehydrogenation samples reveals a lack of the R-space peaks in the 3–6 Å range indicating the lack of ordered metallic structures. Fitting the spectra of both metals using composite models analogous to that used for the Ir model system¹⁴ gives mean 1NN M–M coordination numbers in the 3–4 range. Fitting the EXAFS spectra also gives 1NN R_{M-M} values that overlap, within experimental error, with the corresponding bulk metals for both Co and Ni samples with Al/M ratios of 1.0, but 1NN R_{M-M} values that are *shorter than* the bulk metal M–M distances for both Co and Ni Al/M = 3.0 samples, consistent with greater M–M bonding in these Al/M = 3.0 samples. Fitting the EXAFS spectra also reveal σ^2_{M-M} values that are approximately twice the experimentally determined bulk metal values, indicative of disordered metal clusters. In addition, (vii) the Z-contrast STEM, MALDI MS, and XAFS results all

show that cyclohexene hydrogenation does not significantly change the speciation of the catalyst solutions. Finally, (viii) Hg(0) poisons both Co and Ni catalysts immediately and completely, when Hg(0) is added in the middle of a hydrogenation run. When Hg(0) is added prior to the start of hydrogenation, the degree of poisoning of the Co catalyst is irreproducible, but the Ni catalyst is poisoned immediately, completely, and reproducibly.

The self-consistent interpretation of all results from the complementary techniques used herein is that the transition metal components of catalysts made from either of the industrial precursors Co(neodecanoate)₂ or Ni(2-ethylhexanoate)₂, plus AlEt₃, consist of a combination of M_n clusters with a broad range of sizes and a large degree of structural disorder, plus unreduced, monometallic species, the distribution between the two phases depending on the Al/M ratio. Furthermore, the Hg(0) poisoning results suggest that Ziegler nanoclusters are the most active catalysts in the industrial Ziegler-type hydrogenation catalyst systems (i.e., that the catalysis is heterogeneous, and if one includes M_{≥4} within the definition of heterogeneous). This work expands on the results of others—notably the important studies by Schmidt and co-workers,¹⁷ and Bönemann and co-workers¹⁸—which show transition metal nanoclusters are present in the Co, Pd, Ni, and Pt Ziegler-type systems they studied. The combined results present the best evidence to date that the “Ziegler nanocluster hypothesis” is the correct answer to the ~50-year-old problem of what is the true nature of the industrial Ni-, and presumably also Co-based catalysts. Restated, the notion that industrial Ziegler-type hydrogenation catalysis proceeds via Ziegler nanoclusters is the leading hypothesis going forward to try to disprove.

Much remains to be done, however. Operando spectroscopy studies of the formation of, and catalysis by, both the Ni and Co industrial catalyst systems remain to be accomplished.⁴⁵ A full kinetic study and rate law determination under non-MTL conditions also remain to be done, and it promises to be challenging due to the high rates of these superior catalysts. In addition, the differences regarding the backscattering contribution from M–Al between the EXAFS spectra of the Ir model system (which show the presence of Al)¹⁴ and those of the industrial Co and Ni-based catalysts studied herein (which do not show the presence of Al) are surprising and remain to be explored—is this simply an artifact of the signal-to-noise of the current EXAFS data, or could a M₄H₄ type catalyst for M = Co and Ni explain this discrepancy, for example? Another important difference between the Ir and Co, Ni catalysts is that catalyst aging slows the rates for the Co, Ni catalysts, opposite what is seen for Ir, so that future studies characterizing the aged Co and Ni catalysts is another, important future objective. Furthermore, specific determination of the form(s) taken and role(s) played by the AlEt₃ component, both in the initial synthesis of the catalyst and during catalytic cyclohexene hydrogenation, remain to be fully understood.¹⁹

Despite the work remaining to be done, this investigation of the homogeneous versus heterogeneous nature of Ziegler-type hydrogenation catalysts is significant for at least four reasons: (i) this study examines Co- and Ni-based catalysts made from the actual industrial precursor materials, which make catalysts that are notoriously problematic to characterize;^{2,3} (ii) the Z-contrast STEM results reported herein represent, to our knowledge,³ the best microscopic analysis of the industrial Co and Ni Ziegler-type hydrogenation catalysts; (iii) this study is the first explicit

application of an established method, using multiple analytical methods and kinetics-based studies, for distinguishing homogeneous from heterogeneous catalysis;^{3,6–15} and (iv) this study parallels the successful study of an Ir model Ziegler catalyst system, thereby benefiting from a comparison to those previously unavailable findings,¹⁴ although the greater M–M bond energy, and tendency to agglomerate, of Ir versus Co or Ni are important differences to be noted.⁴⁶ Overall, the main result of this work is that it provides the leading hypothesis going forward to try to refute in future work: namely, that sub, M_{≥4} to larger, M_n Ziegler nanoclusters are the dominant, industrial, Co- and Ni- plus AlR₃ catalysts in Ziegler-type hydrogenation systems.

■ ASSOCIATED CONTENT

S Supporting Information. Experimental information and results of control experiments for cyclohexene hydrogenations used to help establish standard conditions for catalyst preparation and use; additional TEM images; figures showing the MALDI MS results; EXAFS spectra with fits; Hg(0) poisoning control experiments; and a full list of the authors of ref 18d. This material is available free of charge via the Internet at <http://pubs.acs.org>.

■ AUTHOR INFORMATION

Corresponding Author

*E-mail: rfinke@lamar.colostate.edu.

■ ACKNOWLEDGMENT

Work was supported by NSF Grant CHE-0611588 at Colorado State University. MALDI MS were obtained with the expert assistance of Phil Ryan (now deceased) of the Macromolecular Resources Lab at CSU. AIF, JCY and RGN acknowledge support by DOE BES Grant DE-FG02-03ER15476. We thank Nebojsa Marinkovic and Syed Khalid at the NSLS, the use of which was supported by the U.S. Department of Energy, Office of Science, Office of Basic Energy Sciences, under Contract No. DE-AC02-98CH10886. Beamline X18B at the NSLS is supported in part by the Synchrotron Catalysis Consortium, U.S. Department of Energy Grant No DE-FG02-05ER15688. We thank JoAn Hudson of Clemson University for the additional TEM imaging.

■ REFERENCES

- (1) Alley, W. M.; Girard, C. W.; Özkar, S.; Finke, R. G. *Inorg. Chem.* **2009**, *48*, 1114–1121.
- (2) Johnson, K. A. *Polym. Prepr.* **2000**, *41*, 1525–1526.
- (3) Alley, W. M.; Hamdemir, I. K.; Johnson, K. A.; Finke, R. G. *J. Mol. Catal. A: Chem.* **2010**, *315*, 1–27.
- (4) Collman, J. P.; Hegedus, L. S.; Norton, J. R.; Finke, R. G. *Principles and Applications of Organotransition Metal Chemistry*; University Science Books: Mill Valley, CA, 1987.
- (5) Schwartz, J. *Acc. Chem. Res.* **1985**, *18*, 302–308.
- (6) Widegren, J. A.; Finke, R. G. *J. Mol. Catal. A: Chem.* **2003**, *198*, 317–341.
- (7) Lin, Y.; Finke, R. G. *Inorg. Chem.* **1994**, *33*, 4891–4910.
- (8) Aiken, J. D., III; Lin, Y.; Finke, R. G. *J. Mol. Catal. A: Chem.* **1996**, *114*, 29–51.
- (9) Widegren, J. A.; Bennett, M. A.; Finke, R. G. *J. Am. Chem. Soc.* **2003**, *125*, 10301–10310.
- (10) Hagen, C. M.; Widegren, J. A.; Maitlis, P. M.; Finke, R. G. *J. Am. Chem. Soc.* **2005**, *127*, 4423–4432.

- (11) Finney, E. E.; Finke, R. G. *Inorg. Chim. Acta* **2006**, *359*, 2879–2887.
- (12) Jaska, C. A.; Manners, I. J. *Am. Chem. Soc.* **2004**, *126*, 1334–1335.
- (13) Jaska, C. A.; Manners, I. J. *Am. Chem. Soc.* **2004**, *126*, 9776–9785.
- (14) Alley, W. M.; Hamdemir, I. K.; Wang, Q.; Frenkel, A.; Li, L.; Yang, J. C.; Menard, L. D.; Nuzzo, R. G.; Özkar, S.; Johnson, K. A.; Finke, R. G. *Inorg. Chem.* **2010**, *49*, 8131–8147.
- (15) Zahmakiran, M.; Özkar, S. *Inorg. Chem.* **2009**, *48*, 8955–8964.
- (16) Halpern, J. *Inorg. Chim. Acta* **1981**, *50*, 11–19.
- (17) (a) Shmidt, F. K.; Nindakova, L. O.; Shainyan, B. A.; Saraev, V. V.; Chipanina, N. N.; Umanetz, V. A. *J. Mol. Catal. A: Chem.* **2005**, *235*, 161–172. (b) Belykh, L. B.; Titova, Yu. Yu.; Umanets, V. A.; Shmidt, F. K. *Russian Journal of Applied Chemistry* **2006**, *79*, 1271–1277. (c) Nindakova, L. O.; Shmidt, F. K.; Saraev, V. V.; Shainyan, B. A.; Chipanina, N. N.; Umanets, V. A.; Belonogova, L. N.; Toryashinova, D.-S. D. *Kinetics and Catalysis* **2006**, *47*, 54–63. (d) Belykh, L. B.; Goremyka, T. V.; Skripov, N. I.; Umanets, V. A.; Shmidt, F. K. *Kinetics and Catalysis* **2006**, *47*, 367–374. (e) Schmidt, F. K.; Ratovskii, G. V.; Dimitrieva, T. V.; Ivleva, I. N.; Borodko, Y. G. *J. Organomet. Chem.* **1983**, *256*, 309–329.
- (18) Studies by Bönemann and co-workers do not focus on hydrogenation catalysis using Ziegler-type systems, but do demonstrate the synthesis and identification of nanoclusters from Ni or Pt Ziegler-type systems. (a) Bönemann, H.; Brijoux, W.; Brinkmann, R.; Endruschat, U.; Hofstadt, W.; Angermund, K. *Revue Roumaine de Chimie* **1999**, *44*, 1003–1010. (b) Bönemann, H.; Waldöfner, N.; Haubold, H.-G.; Vad, T. *Chem. Mater.* **2002**, *14*, 1115–1120. (c) Angermund, K.; Bühl, M.; Dinjus, E.; Endruschat, U.; Gassner, F.; Haubold, H.-G.; Hormes, J.; Köhl, G.; Mauschick, F. T.; Modrow, H.; Mörtel, R.; Mynott, R.; Tesche, B.; Vad, T.; Waldöfner, N.; Bönemann, H. *Angew. Chem., Int. Ed.* **2002**, *41*, 4041–4044. (d) Angermund, K.; et al. *J. Phys. Chem. B* **2003**, *107*, 7507–7515. (e) Haubold, H.-G.; Vad, T.; Waldöfner, N.; Bönemann, H. *J. Appl. Crystallogr.* **2003**, *36*, 617–620. (f) Wen, F.; Bönemann, H.; Mynott, R. J.; Spliethoff, B.; Weidenthaler, C.; Palina, N.; Zinoveva, S.; Modrow, H. *J. Organomet. Chem.* **2005**, *19*, 827–829.
- (19) Hamdemir, I. K.; Özkar, S.; Johnson, K. A.; Finke, R. G., manuscript in preparation.
- (20) Aiken, J. D., III; Finke, R. G. *J. Am. Chem. Soc.* **1998**, *120*, 9545–9554.
- (21) (a) Lin, Y.; Finke, R. G. *Inorg. Chem.* **1994**, *33*, 4891–4910. (b) Watzky, M. A.; Finke, R. G. *J. Am. Chem. Soc.* **1997**, *119*, 10382–10400. and (c) Widgren, J. A.; Aiken, J. D., III; Özkar, S.; Finke, R. G. *Chem. Mater.* **2001**, *13*, 312–324.
- (22) Kearns, G. J.; Foster, E. W.; Hutchison, J. E. *Anal. Chem.* **2006**, *78*, 298–303.
- (23) (a) Newville, M. J. *Synchrotron Rad.* **2001**, *8*, 322–324. (b) Ravel, B.; Newville, M. J. *Synchrotron Rad.* **2005**, *12*, 537–541.
- (24) Lin, Y.; Finke, R. G. *J. Am. Chem. Soc.* **1994**, *116*, 8335–8353.
- (25) *CRC Handbook of Chemistry and Physics*; 77th ed., Lide, D. R., Frederikse, H. P. R., Eds.; CRC Press: Boca Raton, 1996.
- (26) The number of atoms in a transition metal nanocluster (n) may be estimated making the necessary approximation that the nanoclusters have the same close-packed atomic structure as the bulk metal (either face centered cubic (fcc) or hexagonal close packed (hcp)), and using the following formula: $n = (N_0 \rho (4/3) \pi (D/2)^3) / W$.²⁴ According to this approach, N_0 is $6.022 \times 10^{23} \text{ mol}^{-1}$, ρ is the room temperature density of the pure bulk metal, D is the measured cluster diameter, and W is the atomic weight of the transition metal. For Ni, ρ is 8.90 g/cm^3 , and W is 58.69 g/mol .²⁵ For Co, ρ is 8.86 g/cm^3 , and W is 58.93 g/mol .²⁵ For example, a Ni cluster diameter of 1.3 nm corresponds to Ni_{~100}.
- (27) Starkey Ott, L.; Cline, M. L.; Deetlefs, M.; Seddon, K. R.; Finke, R. G. *J. Am. Chem. Soc.* **2005**, *127*, 5758–5759.
- (28) Hagen, C. M.; Vieille-Petit, L.; Laurency, G.; Süß-Fink; Finke, R. G. *Organometallics* **2005**, *24*, 1819–1831.
- (29) Williams, D. B.; Carter, C. B. *Transmission Electron Microscopy*; Plenum Press: New York, 1996.
- (30) Catalyst samples, both before and after hydrogenation, were also analyzed using bright field and high resolution (HR)TEM as control experiments. Images and a short discussion of those results can be found in the Supporting Information.
- (31) Pyrz, W. D.; Buttrey, D. J. *Langmuir* **2008**, *24*, 11350–11360.
- (32) Whetten, R. L.; Khoury, J. T.; Alvarez, M. M.; Murthy, S.; Vezmar, I.; Wang, Z. L.; Stephens, P. W.; Cleveland, C. L.; Luedtke, W. D.; Landman, U. *Adv. Mater.* **1996**, *8*, 428.
- (33) Khitrov, G. A.; Strouse, G. F. *J. Am. Chem. Soc.* **2003**, *125*, 10465.
- (34) Kuzuya, T.; Tai, Y.; Yamamuro, S.; Sumiyama, K. *Chem. Phys. Lett.* **2005**, *407*, 460–463.
- (35) Maya, L.; Chen, C. H.; Stevenson, K. A.; Kenik, E. A.; Allman, S. L.; Thundat, T. G. *J. Nanoparticle Res.* **2002**, *4*, 417.
- (36) Goulon, J.; Georges, E.; Goulon-Ginet, C.; Chauvin, Y.; Commereuc, D.; Dexpert, H.; Freund, E. *Chem. Phys.* **1984**, *83*, 357–366. (b) Esselin, C.; Bauer-Grosse, E.; Goulon, J.; Williams, C.; Chauvin, Y.; Commereuc, D.; Freund, E. *J. Phys. Colloq.* **1986**, *47*, C8–243–C8–248.
- (37) Frenkel, A. I.; Hills, C. W.; Nuzzo, R. G. *J. Phys. Chem. B* **2001**, *105*, 12689–12703.
- (38) Since much of the other data presented herein is for the Al/Ni = 2.0 catalyst, we carefully considered if it was important to have higher quality data for the Al/Ni = 2.0 sample in order to support the conclusions in the present study. We reasoned that such data are not necessary, primarily on the basis of the following four reasons. First, the XANES spectra of these samples show a smooth progression of the samples from the Al/Ni = 1.0 to Al/Ni = 3.0 ratios. Second, there is considerable similarity between the Al/Ni = 2.0 and 3.0 spectra when plotted as $\chi(k)$, and despite the additional noise apparent in the Al/Ni = 2.0 sample (relevant spectra comparisons are given in the Supporting Information). Third, these first two observations, together with the similarity between the fitting results from catalyst samples with Al/Ni ratios of 1.0 and 3.0, demonstrate that reliable fitting results for the Al/Ni = 2.0 sample should have values between those obtained from the Al/Ni = 1.0 and 3.0 samples. And fourth, the interpretation of the XAFS data herein, that INN M–M coordination numbers are not representative of cluster nuclearity, means that a direct comparison between the results from XAFS and cluster size measurements using other methods such as Z-contrast STEM is not straightforward; this is the case even if higher quality data for the Al/Ni = 2.0 sample were in hand. In short, obtaining higher quality data for the Al/Ni = 2.0 sample is not expected to improve or change any of the conclusions reached in the present study.
- (39) One possible interpretation is that M_{~4-6} clusters remain tightly associated (i.e., (M_{~4-6})_n). For some precedent for this, see: (a) Fulton, J. L.; Linehan, J. C.; Autrey, T.; Balasubramanian, M.; Chen, Y.; Szymczak, N. K. *J. Am. Chem. Soc.* **2007**, *129*, 11936–11949. (b) Harada, M.; Asakura, K.; Toshima, N. *J. Phys. Chem.* **1994**, *98*, 2653–2662.
- (40) (a) Ankudinov, A. L.; Rehr, J. J.; Low, J. J.; Bare, S. R. *J. Chem. Phys.* **2002**, *116*, 1911–1919. (b) Petkov, V.; Ohta, T.; Hou, Y.; Ren, Y. *J. Phys. Chem. C* **2007**, *111*, 714–720. (c) Petkov, V.; Bedford, N.; Knecht, M. R.; Weir, M. G.; Crooks, R. M.; Tang, W.; Henkelman, G.; Frenkel, A. *J. Phys. Chem. C* **2008**, *112*, 8907–8911. (d) Sun, Y.; Zhuang, L.; Lu, J.; Hong, X.; Liu, P. *J. Am. Chem. Soc.* **2007**, *129*, 15465–15467. (e) Vila, F.; Rehr, J. J.; Kas, J.; Nuzzo, R. G.; Frenkel, A. I. *Phys. Rev. B* **2008**, *78*, 121404–1–121404–4. (f) Sanchez, S. I.; Menard, L. D.; Bram, A.; Kang, J. H.; Small, M. W.; Nuzzo, R. G.; Frenkel, A. I. *J. Am. Chem. Soc.* **2009**, *131*, 7040–7054. (g) Gilbert, B.; Huang, F.; Zhang, H.; Waychunas, G. A.; Banfield, J. F. *Science* **2004**, *305*, 651–654. (h) Billinge, S. J. L.; Levin, I. *Science* **2007**, *316*, 561–565. (i) Sun, Y.; Frenkel, A. I.; Isseroff, R.; Shonbrun, C.; Forman, M.; Shin, K.; Koga, T.; White, H.; Zhang, L.; Zhu, Y.; Rafailovich, M. H.; Sokolov, J. C. *Langmuir* **2006**, *22*, 807–816. (j) Menard, L. D.; Xu, H.; Gao, S.-P.; Twisten, R. D.; Harper, A. S.; Song, Y.; Wang, G.; Douglas, A. D.; Yang, J. C.; Frenkel, A. I.; Murray, R. W.; Nuzzo, R. G. *J. Phys. Chem. B* **2006**, *110*, 14564–14573.
- (41) Finke, R. G.; Özkar, S. *Coord. Chem. Rev.* **2004**, *248*, 135–146.
- (42) Yevick, A.; Frenkel, A. I. *Phys. Rev. B* **2010**, *81*, 115451.
- (43) In addition, the explanation of the low XAFS N_{M-M} values involving disordered structure alone requires a degree of N_{M-M}

distortion of considerably greater magnitude than reported in the literature.⁴² The expected, nondistorted, N_{M-M} value for mean 1.4–1.3 nm Co and Ni clusters (determined by Z-contrast STEM) is approximately 8.6–8.9. The observed values from the XAFS results herein, Tables 2 and 3, are decreased by about 50%, as opposed to a disorder-induced decrease in N_{M-M} of 8% calculated in a previous study.⁴²

(44) (a) The potential weaknesses and pitfalls of Hg(0) as a test for the homogeneous versus heterogeneous nature of a catalyst are discussed elsewhere.⁶ (b) Also see Phan, N. T. S.; Van Der Sluys, M.; Jones, C. W. *Adv. Synth. Catal.* **2006**, *348*, 609–679.

(45) (a) Thomas, J. M.; Somorjai, G. A. *Top. Catal.* **1999**, *8* (preface); (b) Weckhuysen, B. M. *Chem. Commun.* **2002**, 97–110. (c) Guerrero-Pérez, M. O.; Bañares, M. A. *Chem. Commun.* **2002**, 1292–1293. (d) Meunier, F.; Daturi, M. *Catal. Today* **2006**, *113*, 1–2.

(46) (a) The standard heats of formation of Ir, Co, and Ni gases are 159.0, 101.5, and 102.7 kcal/mol, respectively.²⁵ This means that at least naked, unligated Ir_n clusters have a greater thermodynamic tendency to agglomerate to the thermodynamic minimum of a bulk Ir(0) mirror compared to Co(0) or Ni(0) clusters. The presence of hydrides or surface ligands, such as in a putative $M_4H_4L_n$, mitigates this driving force some, however, since Ir–H and Ir–L bond energies should be stronger than Co or Ni ones. (b) A useful reference on this point is: Kilic, C. *Solid State Commun.* **2010**, *150*, 2333–2336. (c) The difference in aging effects on the catalysts, the Ir system becoming faster, while aging the Co and Ni catalysts for 24 h has either a slight or significant slowing effect, respectively, (see the Supporting Information) is noteworthy here, and shows an important difference in the Co and Ni versus Ir samples. This difference, in turn, suggests that characterization of the Co and Ni samples as a function of aging is an important future goal—that aged material is *not* the best catalyst.